



## Article

# Forest Structure Characterization in Germany: Novel Products and Analysis Based on GEDI, Sentinel-1 and Sentinel-2 Data

Patrick Kacic <sup>1,\*</sup>, Frank Thonfeld <sup>2</sup>, Ursula Gessner <sup>2</sup> and Claudia Kuenzer <sup>1,2</sup>

<sup>1</sup> Department of Remote Sensing, Institute of Geography and Geology, University of Würzburg, 97074 Würzburg, Germany

<sup>2</sup> German Remote Sensing Data Center (DFD), German Aerospace Center (DLR), 82234 Wessling, Germany

\* Correspondence: patrick.kacic@dlr.de

**Abstract:** Monitoring forest conditions is an essential task in the context of global climate change to preserve biodiversity, protect carbon sinks and foster future forest resilience. Severe impacts of heatwaves and droughts triggering cascading effects such as insect infestation are challenging the semi-natural forests in Germany. As a consequence of repeated drought years since 2018, large-scale canopy cover loss has occurred calling for an improved disturbance monitoring and assessment of forest structure conditions. The present study demonstrates the potential of complementary remote sensing sensors to generate wall-to-wall products of forest structure for Germany. The combination of high spatial and temporal resolution imagery from Sentinel-1 (Synthetic Aperture Radar, SAR) and Sentinel-2 (multispectral) with novel samples on forest structure from the Global Ecosystem Dynamics Investigation (GEDI, LiDAR, Light detection and ranging) enables the analysis of forest structure dynamics. Modeling the three-dimensional structure of forests from GEDI samples in machine learning models reveals the recent changes in German forests due to disturbances (e.g., canopy cover degradation, salvage logging). This first consistent data set on forest structure for Germany from 2017 to 2022 provides information of forest canopy height, forest canopy cover and forest biomass and allows estimating recent forest conditions at 10 m spatial resolution. The wall-to-wall maps of the forest structure support a better understanding of post-disturbance forest structure and forest resilience.

**Keywords:** forest; forest structure Germany; canopy height; Global Ecosystem Dynamics Investigation; GEDI; Sentinel-1; Sentinel-2; random forest regression



**Citation:** Kacic, P.; Thonfeld, F.; Gessner, U.; Kuenzer, C. Forest Structure Characterization in Germany: Novel Products and Analysis Based on GEDI, Sentinel-1 and Sentinel-2 Data. *Remote Sens.* **2023**, *15*, 1969. <https://doi.org/10.3390/rs15081969>

Academic Editors: María Teresa Lamelas, Dario Domingo and Jan Altman

Received: 13 February 2023

Revised: 3 April 2023

Accepted: 6 April 2023

Published: 7 April 2023



**Copyright:** © 2023 by the authors. Licensee MDPI, Basel, Switzerland. This article is an open access article distributed under the terms and conditions of the Creative Commons Attribution (CC BY) license (<https://creativecommons.org/licenses/by/4.0/>).

## 1. Introduction

Europe has experienced severe environmental impacts as a consequence of repeated drought conditions since 2018 [1,2]. A strong link between drought conditions and tree mortality has been reported highlighting the dependency of forest health on the climatic water balance [3]. Among European countries, Germany and Czechia were most heavily affected [4], which is expressed by exceptionally high timber removals to net increment in European forests due to salvage logging [5].

About 32% of Germany is covered by forested areas with a share of coniferous forests of about 55% and deciduous stands of about 45%. The dominant tree species are spruce (25%), pine (23%), beech (16%) and oak (10%). In general, forests are managed as mono-structures in terms of age and tree species richness [6]. The largest forest areas in Germany are located in the federal states of Bavaria (23.4% of the total forest area in Germany), Baden-Württemberg (12.7%), Brandenburg (9.7%) and Lower Saxony (9.7%) (Figure 1) [7]. Nevertheless, the two federal states with the highest shares of forest area related to their federal area are Rhineland-Palatinate (40.7%) and Hesse (39.9%) [7]. There are four types of forest ownership in Germany: federal forest (3% of all forest area in Germany), land forest (32%), corporate forest (22%) and private forest (43%) [8]. Overall, silviculture is an

important industry in Germany [9] with increasing exports until 2021 (e.g., about 50.6% to China in 2020) [10] and significant increments in turnover by about 33% when comparing 2008 to 2018 [11].

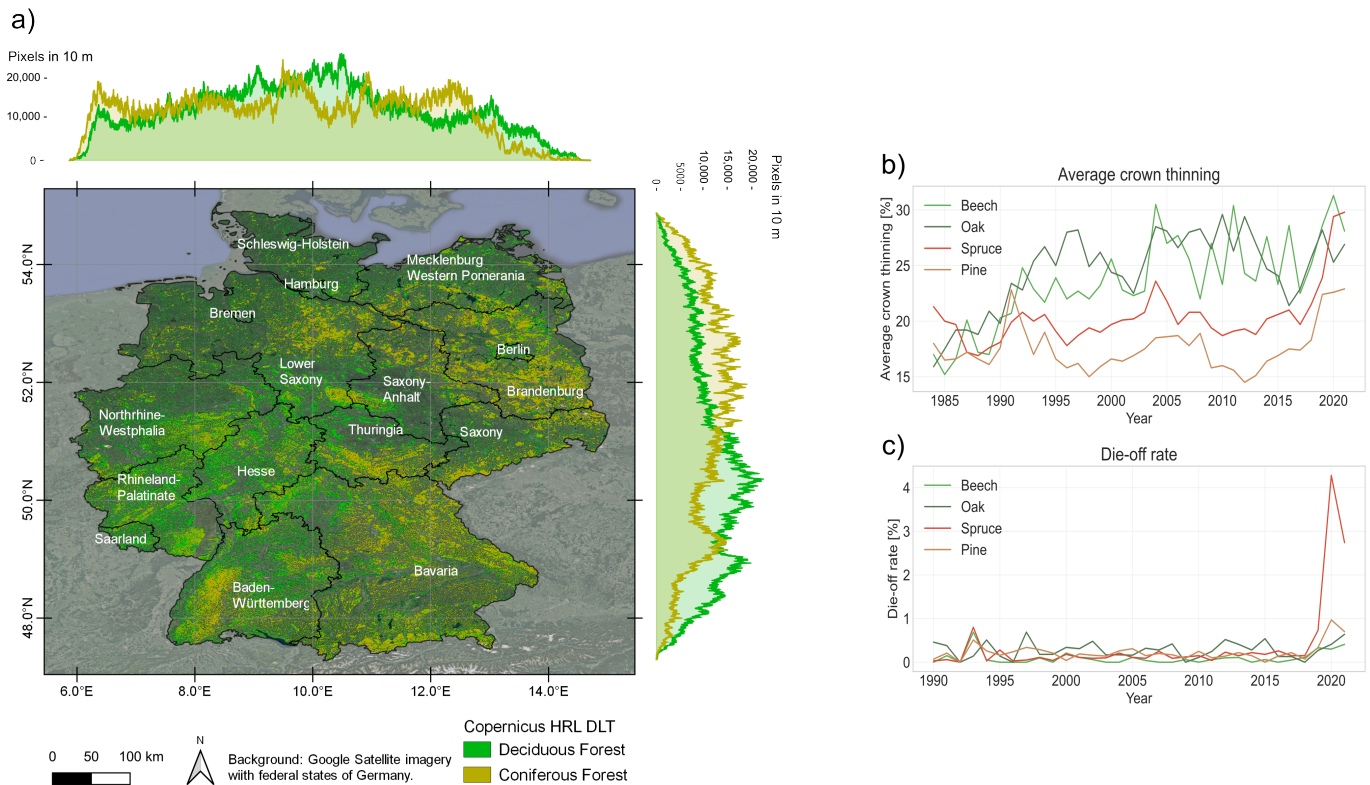


**Figure 1.** General overview on the forest area and forest types (a) according to the Copernicus High-Resolution Layer (HRL) Dominant Leaf Type 2018 (DLT) [12]. In addition, statistics on average crown thinning (b) and die-off rates (c) are displayed based on data from the crown condition survey (Waldzustandserhebung) [13].

In recent years, forests in Germany are increasingly facing extreme wind and weather conditions resulting in different disturbance structures [14]. Heatwaves and droughts reduce the resilience of forests, thus promoting specifically favorable conditions for the spread of insects. Logged timber due to insect infestations from 2016 to 2020 was nearly 13 times more than in 2015 [15]. In 2020, timber logged in consequence of tree damage made up 75% of all harvested timber [15] and further increased in 2021 amounting to 81.4% [16]. The major share of timber cutting due to insect damage is occurring in private forests (56.1%), followed by national forests (23.4%) and corporate forests (20.5%) [16]. The die-off rate grouped by dominant tree species highlights the susceptibility of spruce since 2018 compared to pine, beech and oak trees (Figure 1c) [13]. In addition, all dominant tree species present increasing average crown thinning (Figure 1b), which is a proxy for decreasing resilience being further expressed by declining rates of fructification [17]. As a result of increasing forest disturbances, recent forest conditions are characterized by canopy cover loss and standing deadwood predominantly in spruce stands (Figure 2a,b). Salvage logging as an economically driven silviculture practice has resulted in large-scale unstocked areas promoting soil degradation and altering community compositions in various taxonomic groups (Figure 2c,d) [18].

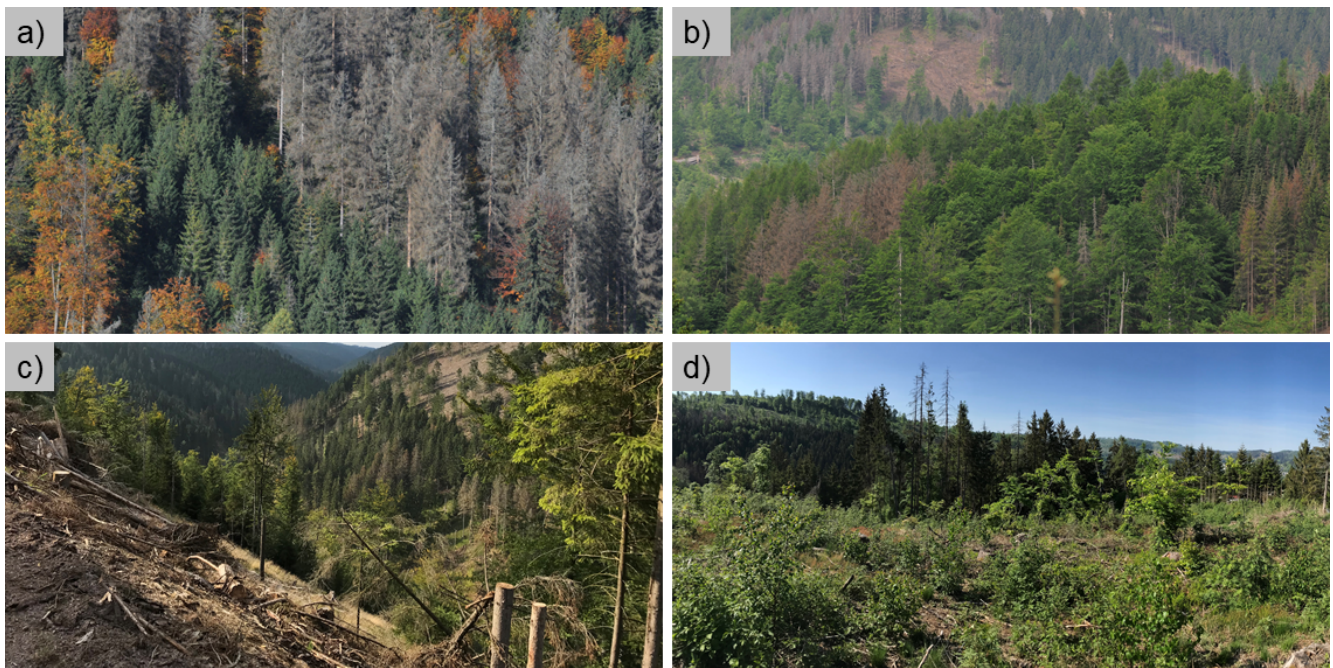


**Figure 2.** Since the drought years 2018 and 2019 there is an increase in canopy cover loss areas (a,b) predominantly in mono-structural spruce stands. In areas of canopy cover loss, salvage logging was a common practice as depicted in the forest areas around Steinach, Thuringia in (c,d). All photos were taken by Frank Thonfeld.

Currently, national forest monitoring systems such as the national forest inventory (Bundeswaldinventur), national forest soil inventory (Bodenzustandserhebung) or crown condition survey (Waldzustandserhebung) are primarily based on sparse sampling grids monitored in long time steps (decadal, approximately 15 years, annual respectively) [17,19,20]. To support future forest resilience, there is the need for consistent monitoring of forest conditions at high spatio-temporal scales. Remote sensing offers cost-effective measurements based on complementary sensors at various platforms bridging information on forest health from in situ to satellite perspectives [21,22]. Multiple large-scale studies demonstrated the accurate assessment of forest disturbance and recovery [23,24]. Recent studies integrating optical imagery confirm drought-induced declines in forest health [25,26]. In particular, the analysis of products combining different remote sensing sensors at high spatial and temporal scale (e.g., Sentinel-1, Sentinel-2, Landsat) have gained in importance and popularity in institutional monitoring systems [12,23,27,28]. Furthermore, Thonfeld et al., 2022 developed a novel product on canopy cover loss areas at monthly resolution for complete Germany from January 2018 until April 2021 combining Sentinel-2 and Landsat 8 imagery [29]. Another recently published study presents a mapping approach of seven dominant tree species for Germany based on Sentinel-2 data [30]. Nevertheless, available products for Germany at high spatial resolution characterizing the three-dimensional structure of forests for an improved understanding of habitats, deadwood structures and biomass pools remain scarce [31–35]. The freely available global products of Potapov et al., 2021 [36] and Lang et al., 2022 [37] have demonstrated the accurate generation of canopy height models integrating novel observations from the Global Ecosystem Dynamics Investigation (GEDI). It is the first spaceborne LiDAR (Light detection and ranging) sensor that is specifically designed to sample vertical and horizontal properties of the Earth’s temperate and tropical forests [38]. The combination of canopy height, canopy cover density, vertical foliage complexity and above-ground biomass density (AGBD) derived from GEDI with wall-to-wall information from mapping missions (e.g., Sentinel-1, Sentinel-2, Landsat) enable the generation of comprehensive data sets on essential biodiversity variables (EBV: AGBD, vegetation height, fraction of vegetation cover) at high spatial and temporal resolution [36,38–40].

The review on forest monitoring in Germany based on earth observation data by Holzwarth et al., 2020 concluded that there is a lack of nationwide studies at multi-temporal scale [19]. Preliminary work on the forest structure of German forests is mainly focused on regional-scale [41–48] or based on coarse resolution imagery [49]. To address these short-comings, the present study builds up on the modeling workflow developed by Kacic et al., 2021 generating data products of complementary attributes of forest structure for the Paraguayan Chaco for a single year (2019) [50]. Therefore, the present study proposes a workflow for the generation of wall-to-wall information on forest structure at 10 m spatial resolution for Germany spanning from 2017 to 2022 based on GEDI, Sentinel-1 and Sentinel-2 data. More in detail, three attributes of the sampling mission GEDI, namely canopy height, total canopy cover and AGBD are modeled as annual products integrating machine-learning regression models based on Synthetic Aperture Radar (SAR) data from Sentinel-1 and multispectral imagery from Sentinel-2. Further objectives of the present study are the general analysis of spatial patterns of forest structure in Germany and the investigation of forest structure dynamics in the context of the drought years 2018 and 2019.

## 2. Materials and Methods

### 2.1. Data and Pre-Processing

The analysis of forest structure in Germany from 2017 to 2022 is based on Sentinel-1, Sentinel-2 and GEDI data. The combination of complementary spaceborne remote sensing data sets from mapping missions (Sentinel-1, Sentinel-2) and sampling missions (GEDI) enables the generation of wall-to-wall products of forest structure. Sentinel-1 Ground-Range-Detected (GRD, 10 m spatial resolution) data were pre-processed analysis ready by applying speckle filtering, radiometric terrain normalization and border noise removal according to Mullissa et al., 2021 [51]. In addition, Sentinel-1 data were filtered to the VV and VH polarization. Data from Sentinel-2 was obtained as surface reflectance product (L2A, processed using sen2cor) [52,53] and further processing steps comprise cloud and cloud shadow masking. In the following analysis of Sentinel-2 data, only the 10 m and 20 m bands are considered. Both Sentinel data sets are derived as annual products from 2017 to including 2022 and are filtered each to the months from April to including September to cover the full vegetation period. All Sentinel pre-processing was conducted in the cloud computing environment of Google Earth Engine (GEE) [54].

GEDI is a full-waveform LiDAR sensor that is attached to the International Space Station (ISS) and operates since April 2019. Following the orbit of the ISS (about 52°N to 52°S), GEDI takes high-resolution measurements of vegetation structure as 25 m footprints within all temperate and tropical forests. The sampling design results in eight ground-tracks with an across-track distance of about 600 m and an along-track distance of about 60 m [38]. In Figure 3, an exemplary subset of 50,000 quality filtered shots of canopy height (GEDI L2A 2021, June to incl. August) are displayed so that the sampling scheme is well presented.

There are three higher-level data sets of GEDI point samples, namely L2A (elevation and height metrics) [55], L2B (canopy cover and vertical profile metrics) [56,57] and L4A (above-ground biomass density, AGBD) [58]. For a comprehensive characterization of forest structure conditions in Germany, data on canopy height (95th percentile of the relative height metrics; official attribute name: rh\_95; L2A product version 2), cover density (total canopy cover; cover; L2B version 2) and biomass (above-ground biomass density; agbd; L4A version 2) was acquired. A detailed overview on available GEDI data for Germany is presented in Table 1. Since GEDI is a LiDAR sensor operating in near-infrared wavelengths, it is sensitive to atmospheric conditions. Therefore, quality filtering for degrade and beam sensitivity was conducted according to best practices: According to general quality flags (L2A: “quality\_flag”; L2B: “l2a\_quality\_flag”, “l2b\_quality\_flag”, L4A: “l2\_quality\_flag”, “l4\_quality\_flag”), low quality shots (value = 0) could be removed. In addition, degraded shots (value > 0) could be filtered out using the “degrade\_flag” and low sensitivity shots (value < 0.95) were removed based on the “sensitivity” attribute [59–61]. For each year

of GEDI data available, a data set of canopy height, total canopy cover and AGBD was generated and temporally filtered to the months of maximum vegetation growth (June to incl. August). At the date of GEDI data processing (November 2022), the most up-to-date GEDI data were from June 2022 which is why the 2022 data set only covers the month June opposing to the other annual products spanning over the months June to incl. August. Quality and temporal filtering of GEDI data were conducted locally (on a virtual machine). Following processing steps of GEDI data were integrated in GEE.

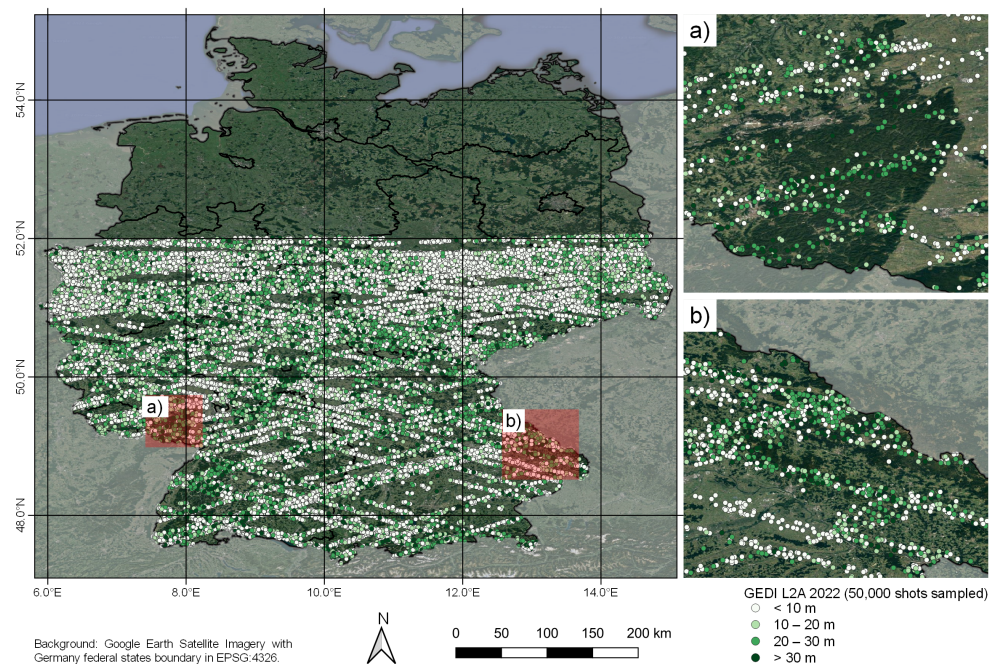


**Figure 3.** Map depicting a subset (50,000 samples for improved visualization) of quality filtered GEDI L2A canopy height data (rh\_95) from 2021 (June to incl. August) for Germany over all land cover types. Since GEDI is attached to the ISS, data acquisition is limited to the northern latitudinal orbit maximum of about 52°N. GEDI measures forest structure in 25 m footprints producing eight transect beams with about 600 m distance in across-track direction and about 60 m distance between footprints in along-track direction (a,b) [38].

**Table 1.** Statistics of quality filtered GEDI data for Germany according to the Algorithm Theoretical Basis Documents (ATBD) [59,60].

GEDI Data Set	L2A	L2B	L4A
<b>Key attributes (official names in brackets)</b>	Relative heights metrics of percentiles (e.g., rh_95; 95th percentile of the relative height metrics)	Canopy height (rh_100), total canopy cover (cover), Plant-Area-Index (pai), Foliage-Height-Diversity-Index (fhd_normal)	Above-ground biomass density (agbd)
<b>Data availability (date: 11 January 2023)</b>	April 2019 to June 2022	April 2019 to June 2022	April 2019 to June 2022
2019	6,924,457	13,938,669	7,612,182
2020	11,432,909	21,130,478	10,514,746
2021	8,638,058	8,717,241	7,233,623
2022	3,935,107	3,545,429	3,287,678

## 2.2. Forest Structure Modeling Workflow

The methodology of the present study builds up on the approach developed in Kacic et al., 2021 combining temporal–spectral metrics of Sentinel-1 and Sentinel-2 to model the first high-resolution maps (10 m) of vegetation structure attributes based on GEDI L2A and L2B data for the dry season 2019 in the Paraguayan Chaco [50]. The present study extends this approach by generating annual products of forest structure information for six years (2017 to incl. 2022) at wall-to-wall coverage (10 m) for Germany. In addition, novel samples of AGBD (GEDI L4A) are added to the analysis for a more comprehensive characterization of forest structure conditions based on canopy height, cover density and AGBD information. Extensive efforts to improve processing performance and avoid exceeding computational limits of GEE revealed that solely using Sentinel-2 band information and training one global annual model for complete Germany based on 10,000 GEDI samples are beneficial updates. Those model simplifications made a workflow possible that does not require a tile-based approach as conducted in Kacic et al., 2021 [50]. Figure 4 depicts the methodological workflow which will be explained more in detail in the following paragraphs.

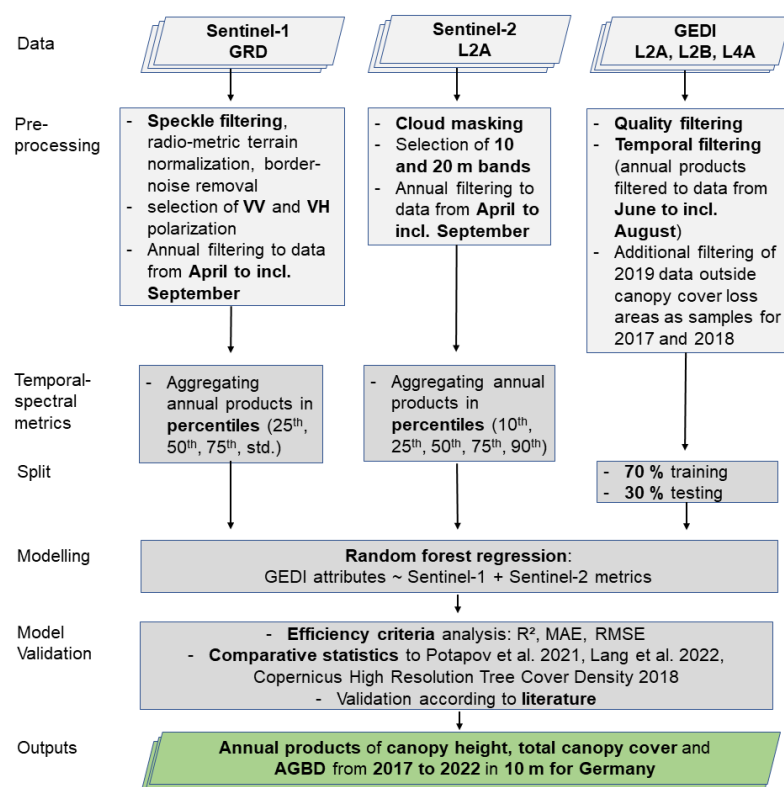


**Figure 4.** Workflow chart of the processing steps of Sentinel-1, Sentinel-2 and GEDI data in order to derive annual wall-to-wall products (10 m) of canopy height, total canopy cover and AGBD from 2017 to 2022 for Germany. The workflow builds up on Kacic et al., 2021 [50] and extends the methodology towards multi-temporal modeling including GEDI L4A data. Comparative statistics are based on Potapov et al. 2021 [36] and Lang et al. 2022 [37].

All the following workflow steps are integrated in GEE for time-efficient processing and simplified transferability of the methodology. Annual products of pre-processed Sentinel-1 data for complete Germany covering the period from April to incl. September (vegetation period) were aggregated in temporal–spectral metrics by calculating percentiles (25th, 50th, 75th) and standard deviation. Similarly, annual Sentinel-2 products at the coverage of Germany from the same temporal period as Sentinel-1 data were reduced to percentile metrics (10th, 25th, 50th, 75th, 90th percentile). The aggregation of time

series satellite data by calculating temporal–spectral metrics (e.g., percentiles) is a common technique [24,36]. Therefore, the influence of gaps in the time series or temporal effects (e.g., atmospheric conditions) are limited although e.g., phenological characteristics are preserved in the temporal–spectral metrics. Furthermore, stacking multi-temporal information is essential to generate a data cube covering large-scale areas [62,63]. In addition to the multi-temporal Sentinel-1 and -2 metrics, mono-temporal elevation information derived from the Shuttle Radar Topography Mission (SRTM) was added to the stack. At the centroid location of GEDI footprints, Sentinel-1 and -2 pixel values were extracted. GEDI samples (10,000 per model) were split in a proportion of training (70%) and testing samples (30%) so that an independent validation of the model according to different efficiency criteria can be conducted. Sentinel and GEDI data were clipped to a mask consisting of the land cover classes “tree cover”, “grassland” and “cropland” from the Worldcover product (2020, 10 m) of the European Space Agency (ESA) [64]. Solely modeling in forested areas would not cover the full range of structural conditions in forests since sparse GEDI samples within forests mainly represent undisturbed conditions whereas GEDI samples within grasslands can approximate canopy cover loss areas.

To derive annual products of canopy height, total canopy cover and AGBD from 2017 to 2022 in 10 m spatial resolution for Germany, for each attribute and each year a random forest model was trained. The random forest regression models with GEDI attributes of forest structure as response variables predicted by Sentinel-1 and -2 temporal–spectral metrics were trained with default settings set in GEE. Random forest models developed by Breiman [65,66] are machine learning models which are commonly applied in remote sensing modeling applications due to their accuracy and performance in the context of high-dimensional data [67,68]. Further, in the modeling applications of GEDI data, random forest regression models are preferred, as conducted in studies based on Landsat [36], Sentinel [50,69] or VIIRS (Visible Infrared Imaging Radiometer Suite) data [70,71]. For the years of GEDI data available (2019 to incl. 2022), the random forest models were trained based on temporal–spectral metrics (annual products) from Sentinel of the corresponding year. Since GEDI data are not available for the years 2017 and 2018, those annual forest structure products were derived by filtering GEDI data from 2019 that is outside canopy cover loss areas detected by Thonfeld et al., 2022 [29] to create a data set of GEDI data that was not affected by disturbances. In the following, those samples were used to train a model based on temporal–spectral metrics from Sentinel-1 and -2 of 2019 which was subsequently applied to separate stacks (2017 and 2018) of temporal–spectral metrics of Sentinel-1 and -2. Similarly to Thonfeld et al., 2022 [29], the rasters of the modeled forest structure were clipped to a combined forest mask consisting of raster data from the Copernicus High Resolution Layer (HRL) Forest Type (FTY) 2015 [27] and vector data from the VEG\_02 layer of the digital landscape model for Germany (DLM250; 1:250,000 scale) [72]. This combined forest mask covers the stocked forest area of Germany.

For model validation of all products (six years; three attributes of forest structure) different model validation techniques were combined. To assess the model accuracy, several efficiency criteria were calculated based on model predictions and independent testing samples: coefficient of determination ( $R^2$ ), Mean Absolute Error (MAE) and Root Mean Square Error (RMSE). For comparative statistics of modeled canopy height, the generated products were compared to the global products of Potapov et al., 2021 [36] and Lang et al., 2022 [73]. The study of Potapov et al., 2021 modeled the 95th percentile of GEDI L2A data for 2019 based on Landsat data in 30 m, whereas Lang et al., 2022 created a canopy height product in 10 m for 2020 based on the 98th percentile of GEDI L2A data. Modeled total canopy cover for 2018 was compared to the Copernicus HRL tree cover density (TCD) layer of 2018 [28]. In a third validation step, modeled forest structure for Germany was validated against literature (e.g., statistics on forest structure based on national forest inventories).

### 3. Results

#### 3.1. Model Accuracy

Model accuracy was calculated for all models based on  $R^2$ , MAE and RMSE (Table 2). According to  $R^2$ , the models of total canopy cover reach highest mean scores of 67.0%. Furthermore, the total canopy cover models hold a mean MAE of 12.5% and RMSE of 19.1%. Modeled canopy height reaches second highest accuracy in mean  $R^2$  (64.6%). There is an error of 4.4 m in MAE and 6.6 m in RMSE. The accuracy for the models of AGBD amount to 58.8% in  $R^2$ , 41.0 Mg/ha in MAE and 64.3 Mg/ha in RMSE. For all years except 2021, the canopy height and total canopy cover models present similar errors according to  $R^2$ , MAE and RMSE. The canopy height models present a  $R^2$  range from 65.3% (2020) to 69.7% (2018) and modeled total canopy cover holds a range from 67.7% (2018) to 68.4% (2017). For both attributes of forest structure, the year 2021 reached comparably lower accuracy, i.e., 56.2% in  $R^2$  for canopy height and 61.5% in  $R^2$  for total canopy cover. Opposing to this finding of one year with a decline in model accuracy, the models for AGBD of 2021 ( $R^2$ : 50.9%) and 2022 ( $R^2$ : 54.7%) present lower accuracy than the AGBD models of 2017 to 2020 ( $R^2$  range: 61.1.% to 62.8%).

For a comparative analysis of modeled forest canopy height in Germany, the results of the present study (2019, 2020) were compared to global products of canopy height by Potapov et al., 2021 (reference year: 2019) [36] and Lang et al., 2022 (reference year: 2020) [37]. Modeled total canopy cover density for 2018 was compared to the Europe-wide product HRL TCD from the European Environment Agency (EEA, reference year: 2018). Figure 5 depicts the results of the comparative analysis.

The validation of the 2019 canopy height models (both modeling the 95th percentile of the GEDI L2A relative height metrics) presents a general agreement of the two products amounting to a MAE of 3.3 m. In comparison, the canopy height analysis for 2020 presents a stronger difference (MAE: 5.2 m) between the product of the present study (95th percentile of the GEDI L2A relative height metrics) and the global product of Lang et al., 2022 (98th percentile of the GEDI L2A relative height metrics) [37]. Modeled forest canopy cover density deviates by 23.9% in MAE when comparing HRL TCD [28] (solely based on Sentinel-2 data) to the total canopy cover product of the present study. The Pearson correlation coefficient of 0.73 indicates a relative high correlation between the two products although there is an offset detected since maximum values of the present study amount to about 80% compared to about 100% in the HRL TCD product.

**Table 2.** Model accuracy assessment for the canopy height, total canopy cover and AGBD models of all years according to the coefficient of determination ( $R^2$ ), Mean Absolute Error (MAE) and Root Mean Square Error (RMSE).

GEDI Attribute	Canopy Height (rh_95)			Total Canopy Cover (Cover)			Above-Round Biomass Density (Agbd)		
	$R^2$ [%]	MAE [m]	RMSE [m]	$R^2$ [%]	MAE [%]	RMSE [%]	$R^2$ [%]	MAE [Mg/ha]	RMSE [Mg/ha]
2017	66.9	4.1	6.5	68.4	11.6	18.3	61.1	41.2	65.3
2018	69.7	4.2	6.2	67.7	11.8	18.5	62.8	38.8	61.3
2019	66.5	4.3	6.6	68.3	11.8	18.4	61.3	40.6	63.7
2020	65.3	4.2	6.5	68.2	11.8	18.4	61.9	38.3	60.2
2021	56.2	5.1	7.7	61.5	14.5	21.2	50.9	47.7	73.0
2022	65.7	4.3	6.3	67.7	13.3	19.7	54.7	39.5	62.4
Mean	64.6	4.4	6.6	67.0	12.5	19.1	58.8	41.0	64.3

To better understand the variable importance of predictor features, the scores for the 2022 canopy height model are depicted in Figure A3. Spectral information of Sentinel-2 in the Red Edge 1 wavelength (B5) holds highest importance scores. Elevation information derived from SRTM is ranked as 6th highest variable, in contrast to Sentinel-1 metrics



reaching lowest scores. The sensitivity analysis for the 2022 canopy height model presents highest model accuracy based on a high number of trees, low minimum leaf population and a rather low number of variables per split (Figure A4).

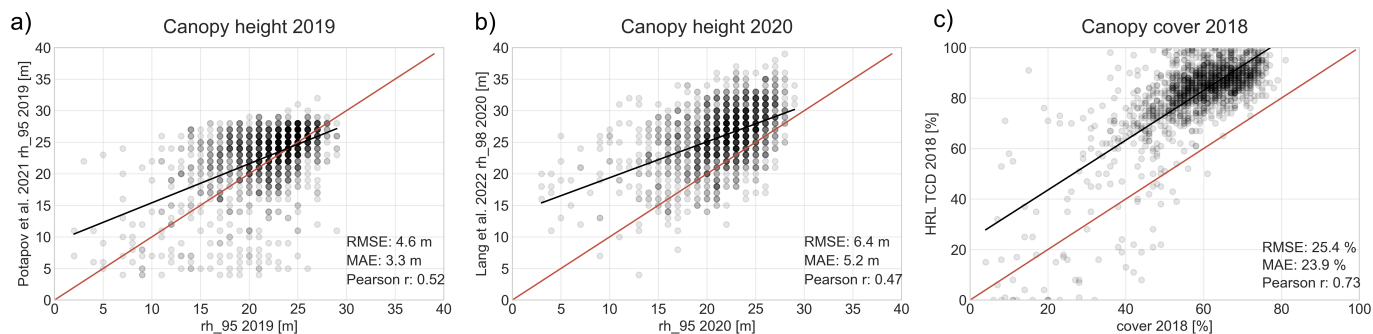


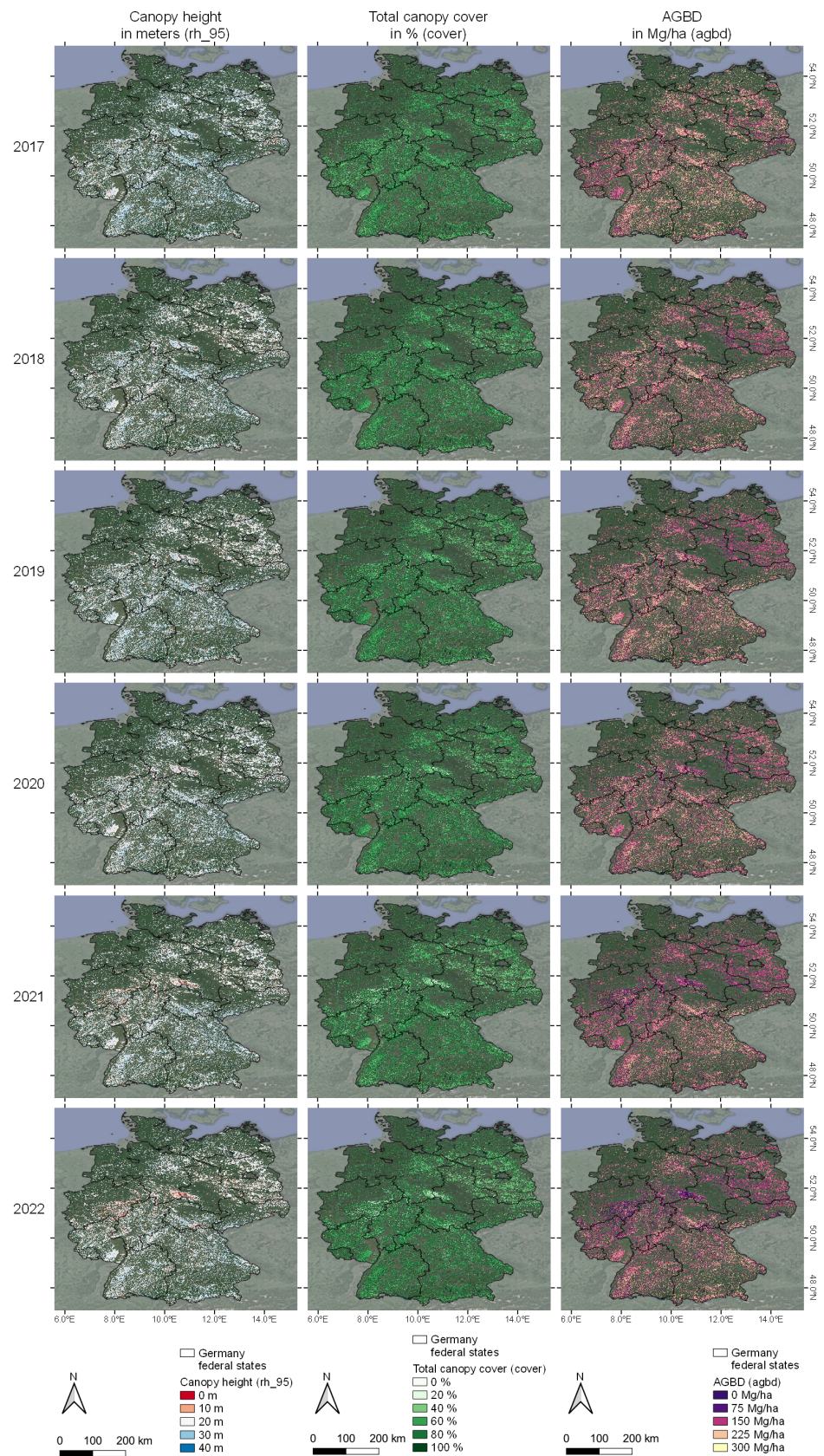
**Figure 5.** Comparison of modeling products from the present study (x-axes) with canopy height models from Potapov et al., 2021 (a) [36] and Lang et al., 2022 (b) [37]. Potapov et al., 2021 modeled canopy height as the 95th percentile from GEDI L2A 2019 data, whereas Lang et al., 2022 generated a canopy height model for 2020 based on the 98th percentile. The total canopy cover product was compared to the Copernicus HRL tree cover density (TCD) layer [28] (c). Model validation is based on 1500 samples that were randomly generated in forested areas lower than 52°N (northern latitudinal limit of Potapov et al., 2021 product [36]).

### 3.2. General Forest Structure Conditions in Germany

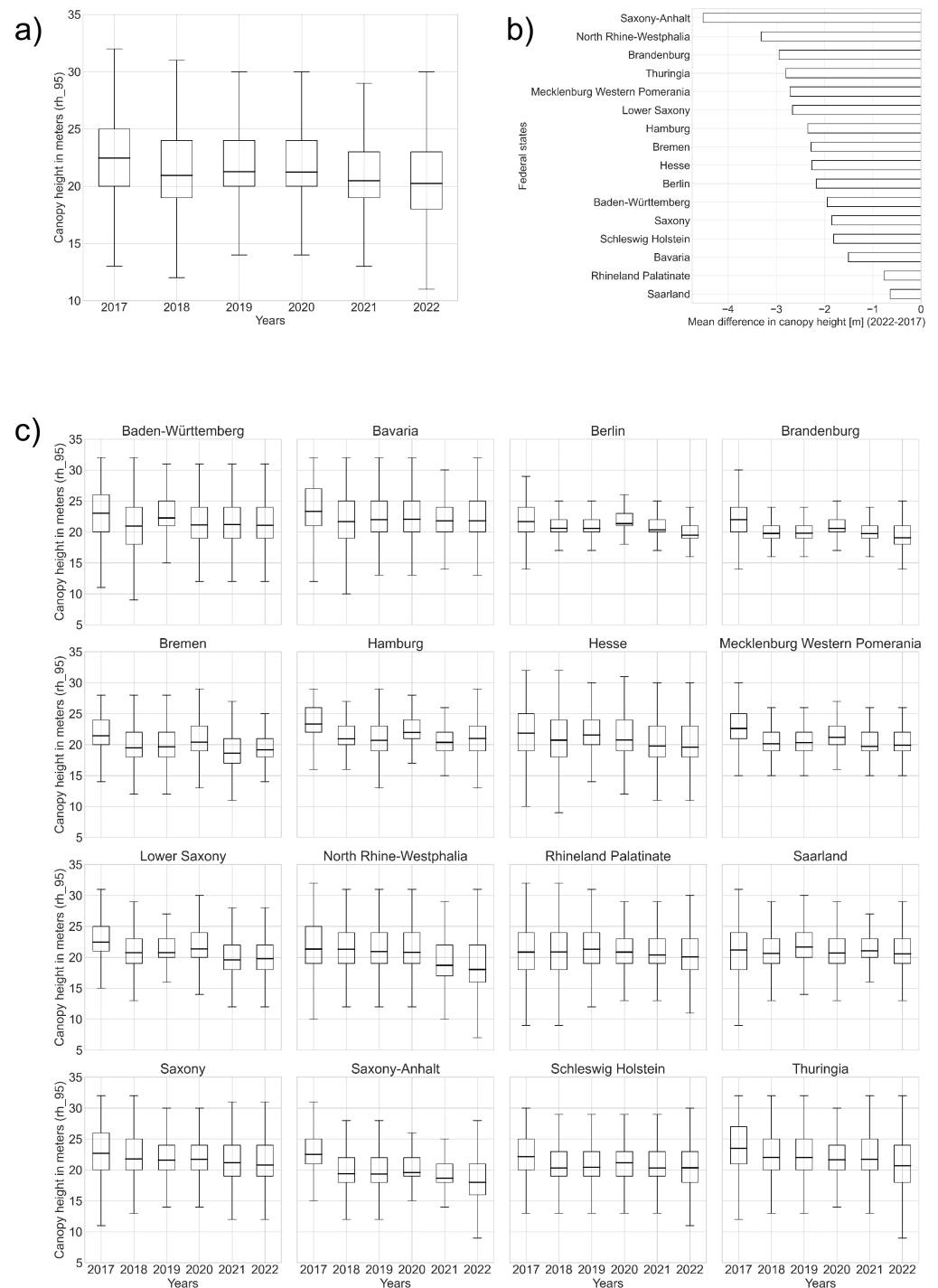
The forest structure conditions in Germany present varying spatial patterns and temporal dynamics. Overall, major large-scale changes in forest structure have been occurring since 2021 (Figure 6). Dominant areas of change in forest structure are canopy cover loss areas in central and western Germany. Those areas are characterized by strong declines in canopy height from greater than 20 m in 2017 to lower than 10 m in 2022. Similarly, there is a temporal gradient in total canopy cover from 2017 to 2022 describing continuous opening of canopy cover density resulting in total canopy cover values lower than 20% in 2022. Those dynamics are also visible in the maps of AGBD for the Harz region since those forests cover a larger, less fragmented area than the forests in Siegen-Wittgenstein. Initial AGBD stocks in 2017 of greater than 225 Mg/ha are dropping to values of lower than 100 Mg/ha in 2022.

Figure 7 presents quantitative statistics of canopy height in Germany. Statistics at the coverage of Germany (Figure 7a) indicate a decline in mean canopy height from 2017 to 2022 depicted by the horizontal line in the boxplots. The mean canopy height in 2017 amounts to about 22.5 m and decreases to about 21 m (2018–2020) and further declines to about 20 m (2021, 2022). Furthermore, there is an increased proportion of low canopy heights in 2021 and 2022: The quartile group one spanning from the minimum to the first quartile (about 25% of all values) presents a range from 13 to 19 m (2021) and 11 to 18 m (2022). Mean difference statistics (Figure 7b) and multi-temporal change in canopy height (Figure 7c) highlight major losses in canopy height in Saxony-Anhalt (mean difference between 2022 and 2017:  $-4.8$  m) and North Rhine-Westphalia ( $-3.2$  m). Rather stable conditions are present in Rhineland-Palatinate and Saarland indicated by a mean difference in canopy height (2022–2017) of greater than  $-1$  m.

In general, the analysis of quantitative statistics of AGBD reveals similar results as found for canopy height, since a steady decline in mean values at the country-level from 2017 to 2022 (195 to 165 Mg/ha) is observed (Figure A2a). In addition, a growing proportion of low AGBD areas is described by an increasing quartile group one in 2022 (75 to 150 Mg/ha, Figure A2b). The federal states with major losses in AGBD (mean difference in AGBD of lower than  $-30$  Mg/ha comparing 2022 to 2017) are Saxony-Anhalt, North Rhine-Westphalia, Mecklenburg Western Pomerania, Thuringia and Brandenburg (Figure A2c).



**Figure 6.** Forest structure from 2017 to 2022 for Germany. The forest areas in the center and western parts of Germany present a declining overall forest structure, i.e., low canopy heights, sparse canopy covers and low AGBD in 2022.



**Figure 7.** Quantitative statistics of canopy height in forested areas of Germany: Overall dynamics in canopy height in Germany (a), mean difference in canopy height (202-2017) among federal states (b), multi-temporal change in canopy height grouped by federal states (c). The statistics are based on predicted pixel estimates depicting mean values as horizontal line in the boxplots. General dynamics of forest structure are assessed; absolute values should be interpreted in the context of model uncertainty.

Opposing to the findings from the quantitative statistics of canopy height (Figure 7) and AGBD (Figure A2), total canopy cover presents relatively stable mean values from 2017 to 2022 ranging from about 55 to 60% (Figure A1a). Similarly to canopy height and

AGBD, total canopy cover presents an increasing proportion of open canopy areas in 2021 and 2022 since about 25% of the forests in Germany hold total canopy cover values in a range from about 20 to 50% (Figure A1a). The statistics of total canopy cover in federal states (Figure A1b,c) present contrasting dynamics of canopy cover density. On the one hand, there are strong losses indicated by a mean difference between 2022 and 2017 of lower than -5% in Saxony-Anhalt and Brandenburg. On the other hand, the federal states of Rhineland-Palatinate and Saarland present increasing cover densities described by a gain in total canopy cover from 2017 to 2022 of greater than 7%.

To sum up, there are strong changes in forest structure in Germany from 2017 to 2022 resulting in increasing proportions of low canopy heights, sparse canopy covers and decreased AGBD. Furthermore, a generalized latitudinal gradient can be observed: Federal states in the northern and central part of Germany (Saxony-Anhalt, Brandenburg, North Rhine-Westphalia and Thuringia) present stronger losses in canopy height, total canopy cover and AGBD than the southern federal states Saarland, Rhineland-Palatinate, Baden-Württemberg and Bavaria. Model uncertainty (Table 2, Figure 5) should be considered, thus limiting the validity of absolute values.

### 3.3. Exemplary Forest Structure Dynamics

In the following, three regional examples of forest structure dynamics in Germany are assessed. First, the Harz region which is a large-scale forest area with comparably low forest fragmentation in 2017 (Figures 8–10). In comparison, the second exemplary region of Siegen-Wittgenstein is characterized by small forest fragments (Figure 11). Both regions presented healthy stands in the pre-drought year 2017 and experienced canopy cover loss through cascading effects of bark beetle infestation and salvage logging as a result of the droughts in 2018 and 2019. As a third example of forest structure dynamics, the region of the Dannenröder Forst in Hesse is analyzed presenting relatively stable conditions in forest structure until 2020 followed by forest loss and forest fragmentation for the construction of the highway A49 which was accompanied by strong protests of conservation initiatives [74] (Figure 12).

Since 2017 there have been dramatic changes in forest structure in the Harz region (Figure 8). Initial conditions in 2017 present a continuous forest coverage with canopy heights of up to 30 m and total canopy cover densities exceeding 80%. In the following years until including 2020 a step-wise spread of areas with reduced forest structure, i.e., canopy heights lower than 10 m and total canopy cover densities below 20% can be observed. Similarly, an area with low AGBD (below 100 Mg/ha) in the north-western part is expanding towards east and south. Since the year 2021, a major proportion of the Harz region has changed to low canopy heights, open canopy covers and reduced AGBD. Overall, there are strong positive correlations between the different attributes of forest structure in areas of canopy cover loss, generally describing the complete loss of stocked forest, i.e., not only of dense canopy cover.

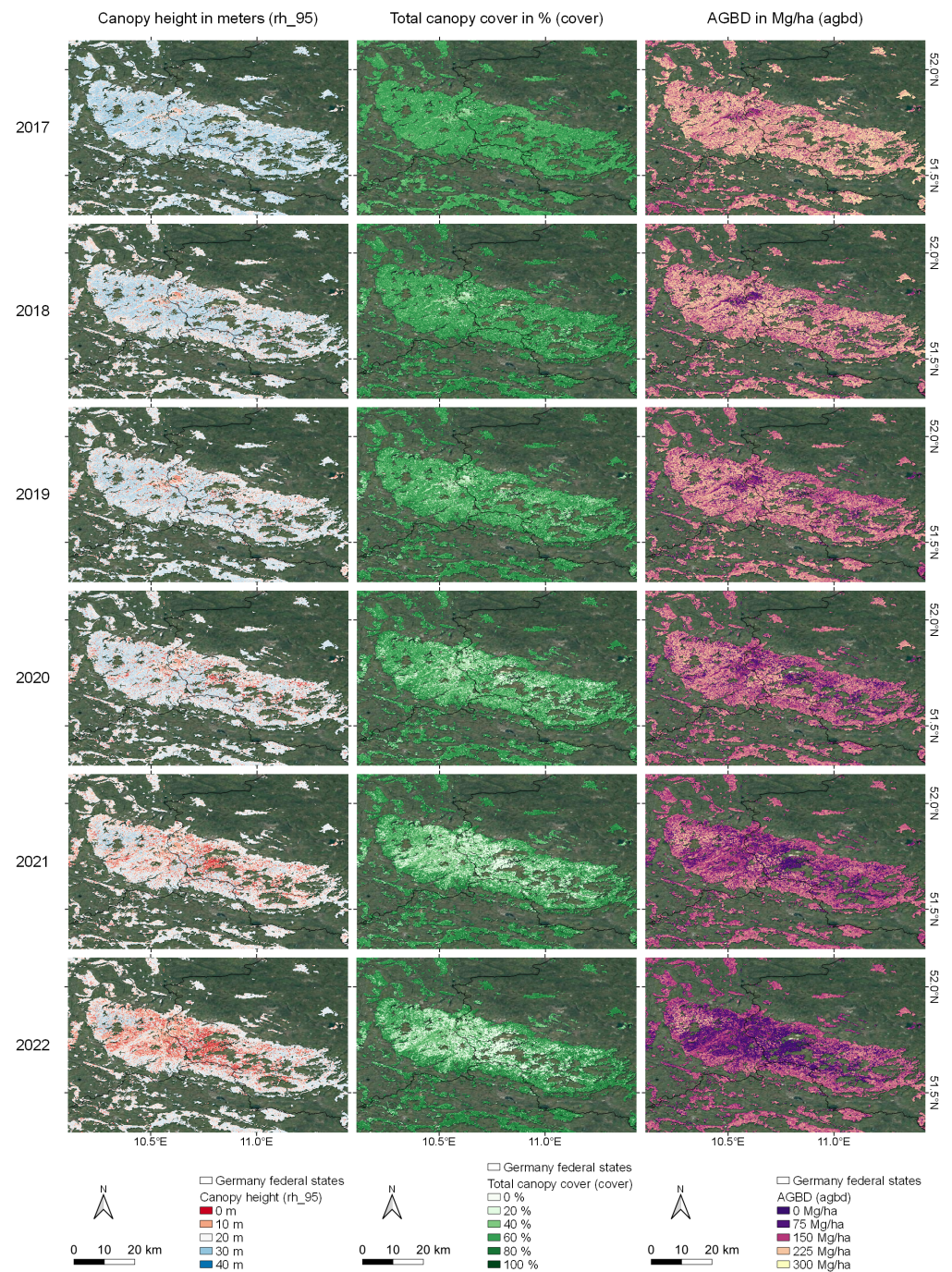


**Figure 8.** Forest structure change in the Harz region (2017 to 2022) presenting massive changes in forest structure since 2018.

To highlight the changes in forest structure from 2017 to 2022, the difference (2022–2017) was calculated for the three attributes of forest structure and compared to canopy cover loss areas (January 2018 to April 2021) [29] and the dominant leaf type (DLT, 2018) product from the Copernicus HRL data sets [12] (Figure 9). In general, the bi-temporal change products of canopy height, total canopy cover and AGBD match the spatial patterns of canopy cover loss assessed by Thonfeld et al., 2022 [29]. Furthermore, the comparison with the HRL DLT product highlights the occurrence of decreased canopy height, cover density and AGBD predominantly in coniferous forests.

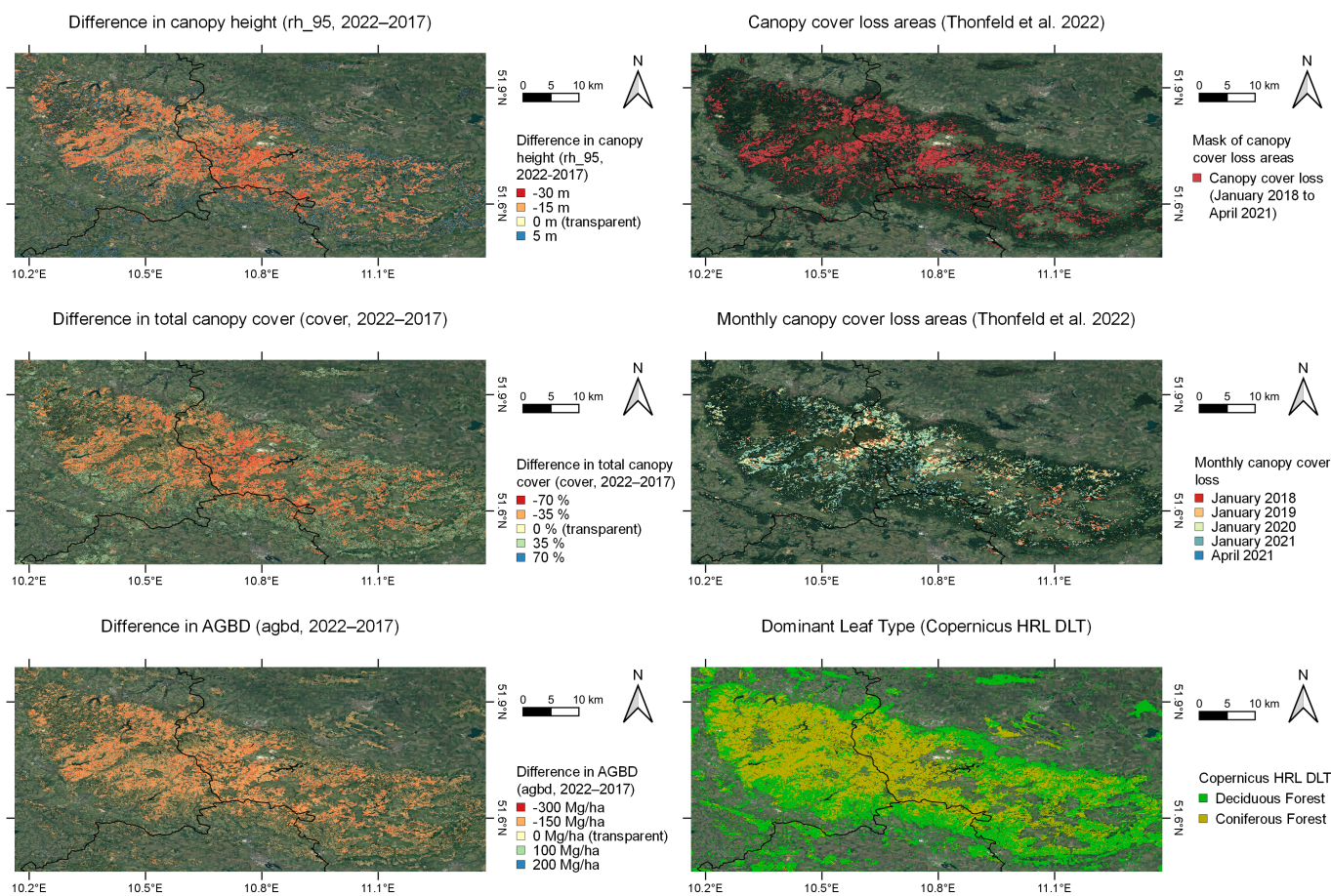


**Figure 9.** Difference in forest structure (2022–2017) in the Harz region reveals corresponding spatial patterns in canopy cover loss areas detected by Thonfeld et al., 2022 [29].

In Figure 10, the three attributes of forest structure are stacked as RGB visualization. For a normalized visualization, all three layers were rescaled to values from 0 to 255. By stacking the three complementary attributes, different spatio-temporal dynamics of canopy height, total canopy cover and AGBD are emphasized: In 2017, there is a dominance of light colors indicating high values in canopy height (red areas), total canopy cover (green areas) and AGBD (blue areas). From 2018 to including 2020, coniferous areas are depicted in light red colors highlighting a loss in cover density and AGBD opposing to canopy height. The year 2021 is characterized by a darkening in red areas, i.e., a further loss in total canopy cover and AGBD accompanied by declining values in canopy height. In 2022, vast areas of the Harz region are covered in black colors indicating low values in all attributes of forest structure. Furthermore, the spatial spread of areas of low canopy height, sparse canopy covers and reduced AGBD (black areas) can be reconstructed since the initial location of forests with those characteristics was in the north-western part of the Harz at the border of Lower Saxony and Saxony-Anhalt expanding predominantly towards south-east. The surrounding deciduous forest presents light green colors in all years thus highlighting much more stable conditions than the adjacent coniferous forests. To sum up, the stacked multi-temporal presentation of canopy height, total canopy cover and AGBD reveals different spatio-temporal dynamics with earlier declines in total canopy cover and AGBD compared to canopy height thus suggesting the occurrence of standing deadwood.

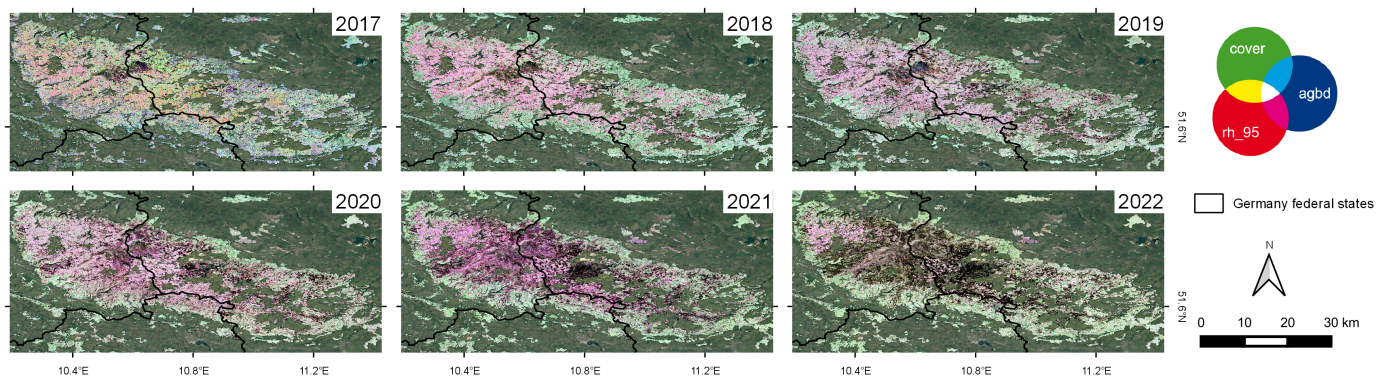


**Figure 10.** Forest structure change in the Harz region visualized as RGB image (red:rh\_95, green:cover, blue:agbd). The visualization as RGB serves as combined visualization of canopy height, total canopy cover and AGBD as annual composites to emphasize the asynchronous temporal dynamics in forest structure. Before stacking the layers, each attribute of forest structure was rescaled to values from 0 to 255 so that the attributes can be compared visually, i.e., to remove scale-dependency. Light colors present high values for all forest structure attributes (e.g., 2017) compared to dark colors (e.g., 2022) which represent low values in the attributes of forest structure. The dominance of a single color (e.g., red in 2018–2021) in large areas highlights comparably high values in canopy height, i.e., losses in total canopy cover and AGBD. The presence of black areas in 2022 presents low overall forest structure, i.e., low canopy height, total canopy cover and AGBD.

The forest areas in the region of Siegen-Wittgenstein are much more fragmented and heterogeneous in size and dominant tree species than the forests in the Harz region. Similar to the Harz region, the years from 2017 to including 2020 present slower dynamics in canopy cover loss than the following years (Figure 11). Only in the central and western areas of Siegen-Wittgenstein, strong declines in canopy height, total canopy cover and AGBD can be observed. Since 2021 large-scale change dynamics in forest structure are taking place: Strongest changes characterized by declines in all forest structure attributes are depicted in the central and south-western areas. Interestingly, a spatial trajectory from north-east to south-west highlights a connectivity of the areas with overall decreased forest structure conditions.

The exemplary forest structure dynamics in the Dannenröder Forst located in the central part of Hesse generally follow the spatio-temporal patterns examined in the Harz and Siegen-Wittgenstein region (Figure 12). In addition, it serves as an example of forest loss and landscape fragmentation in Germany due to infrastructure construction [74]. For the construction of the highway A49, forest clearing and logging took place in winter 2020 which is why the years before including 2020 present pre-construction conditions. The products of modeled forest structure of 2021 and 2022 clearly indicate the complete removal of trees as depicted by the linear features in the western part.

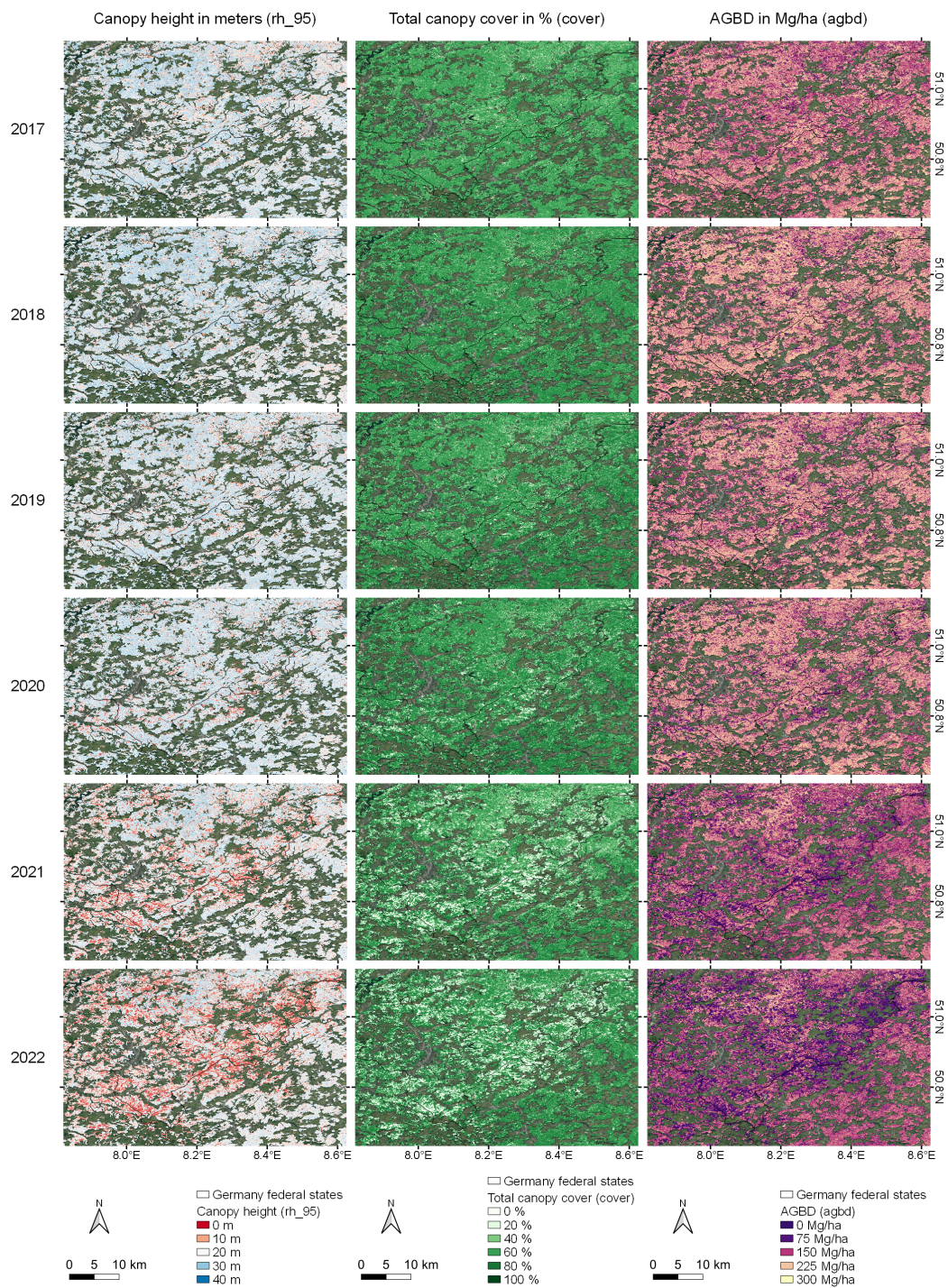


**Figure 11.** Forest structure change in the Siegen-Wittgenstein region (2017 to 2022). Major changes are taking place in 2021 and 2022 as the result of large-scale salvage logging in coniferous stands.



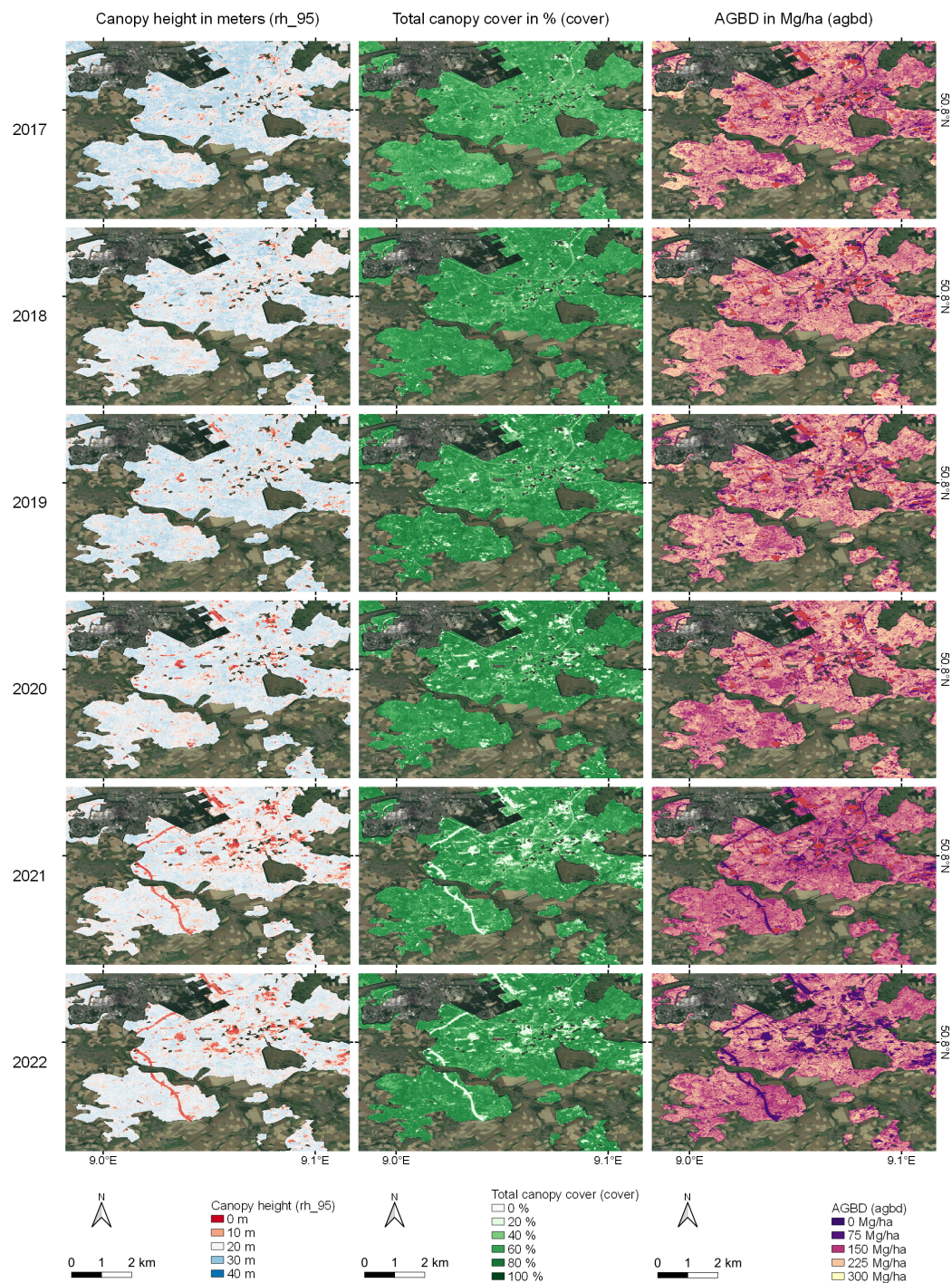


**Figure 12.** Forest structure change in the Dannenröder Forst (2017 to 2022). Rather stable conditions until 2020 are followed by logging activities resulting forest loss and forest fragmentation for the construction of the highway A49.

#### 4. Discussion

The developed methodology for generating multi-temporal products of complementary forest structure attributes for Germany presents relatively similar model accuracy estimates for all years thus allowing for a comparability of models. A decreased model accuracy in 2021 could be influenced by a lower number of Sentinel-2 scenes with a low cloud-coverage available for 2021 (2602 scenes, maximum cloud-coverage threshold for all years: 60%). In comparison, the other years with both Sentinel-2A and Sentinel-2B available

present a higher number of scenes (2018: 3579, 2019: 3113, 2020: 3488, 2022: 2914). The mean  $R^2$  of the canopy height models amounting to 64.6% indicates a similar or higher model accuracy than other studies modeling GEDI-derived canopy height. Potapov et al., 2021 presented the first global product of canopy height derived from GEDI and Landsat imagery reaching a  $R^2$  value of 61.0%. The study of Sothe et al., 2022 modeling canopy height for Canada based on a multi-sensor approach (GEDI, ICE-Sat-2, PALSAR, Sentinel-1, Sentinel-2) achieved 58.0% in  $R^2$  [69]. Modeled canopy height for the Paraguayan Chaco based on GEDI, Sentinel-1 and -2 amounts to 64.0% in  $R^2$  [50]. More detailed statistics comparing the global canopy height product of Potapov et al., 2021 with the national canopy height product for 2019 of the present study show a general agreement of the two products expressed by a MAE of 3.3 m. Strongest differences between the products are observed in the range from modeled canopy height between 15 to 25 m (Figure 5a). An influential factor on the statistics could be the difference in spatial resolution since the product of Potapov et al., 2021 [36] is published in 30 m whereas the product of the present study comes in 10 m. The comparative statistics of the global canopy height product from Lang et al., 2022 [37] reveal a stronger difference although both studies integrate Sentinel-2 data (Figure 5b). One plausible reason for the systematic positive offset of the product from Lang et al., 2022 [37] compared to modeled canopy height for 2020 of the present study could be the choice of different percentiles from the GEDI L2A relative height metrics: Lang et al., 2022 obtained the 98th percentile opposing to the present study integrating the 95th percentile. The validation of modeled total canopy cover could not be accomplished based on a reference product also integrating GEDI L2B data since such a product is not yet published. Therefore, data from the HRL TCD product were obtained although it is solely based on Sentinel-2 data [28] and hence does not consider LiDAR-derived information on cover density. The deviation of 23.9% in MAE between the two products assessing canopy cover density and the different value ranges (HRL TCD: 0 to 100%; modeled total canopy cover: 0 to 80%) highlight a general offset towards underestimation of canopy cover closure when integrating spaceborne LiDAR-derived information compared to multispectral imagery (Figure 5c).

Overall, the generated forest structure products confirm different dynamics present in the forests of Germany: Large-scale salvage logging dynamics in the region of Siegen-Wittgenstein (Figure 11), the continuous spread of sparse canopy covers accompanied by reduced AGBD in the Harz region (Figure 10) and forest fragmentation through infrastructure construction in the Dannenröder Forst (Figure 12). Therefore, major changes in forest condition can be characterized based on the annual products of canopy height, total canopy cover and AGBD spanning from 2017 to 2022. Those findings are aligned with statistics from national forest inventories: Strong differences in forest structure between 2017 and 2022 as explained for the spruce-dominated Harz region (Figures 8–10 are confirmed by time-series information on average crown thinning and die-off rates [13,17] (Figure 1b,c). Besides drought-related disturbances, also winter storms (e.g., Friederike in January 2018) caused severe damage to the forests in central Germany [75]. Large-scale salvage logging as conducted in the region of Siegen-Wittgenstein described by strong declines in all modeled attributes of forests structure (Figure 11) has also been reported by national statistics highlighting insects as primary cause [15,16]. Therefore, the products of modeled forest structure enable an analysis at high spatial resolution for complete Germany within the range of model accuracy hence limiting the validity of minor gradients of change. Nevertheless, aforementioned major change dynamics are accurately assessed in space and time suggesting a consistency in relative forest structure over time.

There are known sensor limitations of GEDI which have been assessed by Adam et al., 2020 [76] validating ground elevation and canopy height estimates based on airborne laser scanning (ALS) data in temperate forests of Thuringia [76]. One main finding is that ground elevation heights are accurately measured ( $R^2$  greater than 93%) if the terrain slope is rather low (strong differences to ALS data if the slope is greater than  $20^\circ$ ). GEDI-derived canopy height measures present lower accuracy ( $R^2$ : 27 to 34%) being more sensitive to different

environmental configurations (slope, vegetation height) and sensor characteristics (beam sensitivity). It should be noted that about 9 to 13% of all ground elevation and canopy height measurements are outliers, thus requiring accurate quality filtering [59,60,76]. The study of Roy et al., 2021 analyzing the geolocation accuracy of GEDI canopy height estimates in a tropical forest ecosystem in the western Democratic Republic of Congo emphasizes the influence of geolocation uncertainty (quality requirement of maximum 10 m in standard deviation) with respect to the 25 m footprint of GEDI. Simulations of horizontal positional errors have been assessed indicating limitations in the validity of canopy height estimates in spatially heterogeneous canopy structures (e.g., forest edges, forest islands) [77]. It should be noted that the studies of Adam et al., 2020 [76] and Roy et al., 2021 [77] are based on the first version release of GEDI data. Therefore, there is no information yet available on the geolocation uncertainty of second version GEDI data which is expected to reach higher geolocation accuracy [77]. A more recent study of Wang et al., 2022 assessing the accuracy in relative height and ground elevation obtaining data from the second version of GEDI L2A data confirms high accuracy of both ground elevation (RMSE: 1.4 m) and canopy height (2.6 m). The study further reports a general underestimation in the relative height metrics and overestimation of the ground elevation compared to airborne LiDAR among various forest types in the United States [78]. Hirschmugl et al., 2023 conducted an analysis of vertical forest structure complexity in the Austrian Alps integrating GEDI L1B and L2B data. The authors highlight the value of information on vertical foliage layering to assess different forest structure groups which is similarly to the findings of aforementioned studies limited by complex terrain and dense vertical layering. Furthermore, GEDI only performed slightly worse to ALS for the separation of vertical foliage layering [79].

Because GEDI data are only available since April 2019, the models of forest structure for 2017 and 2018 are based on GEDI shots from 2019. To account for the temporal mismatch and avoid the influence of disturbance in 2018, the GEDI data were filtered to non-canopy cover loss areas according to Thonfeld et al., 2022 [29]. In addition, one model for each attribute of forest structure was trained based on a stack of Sentinel data from 2019, which was in the next step applied to separate wall-to-wall stacks of Sentinel features for 2017 and 2018. Therefore, the temporal transferability of the 2019 model is valid under the assumption of spectral and spatial consistency of the Sentinel data [80]. The assessment of the model performance confirms this assumption since modeling accuracy for 2017 and 2018 is similar or higher than years with a temporal match of GEDI and Sentinel data (Table 2). Rishmawi et al., 2022 integrated a similar modeling framework by training a model combining GEDI L2B (2019–2020) and VIIRS (2019) data, which was applied to VIIRS stacks from 2013 to 2020 to predict forest structure dynamics for the United States [71].

The generated products of forest structure of the present study cover the complete land area of Germany although GEDI data were limited by its orbit to about 52°N [38]. Therefore, predictions for the areas north of about 52°N should be interpreted with caution. Nevertheless, since the forest structure of Germany is dominated by few main species that are both present north and south of 52°N, there are no strong gradients of change in dominant tree species [6,30]. Similarly, environmental conditions such as climate do not present major differences between northern Germany in comparison to central and southern Germany [81,82].

Overall, the annual products on canopy height, total canopy cover and AGBD from 2017 to 2022 serve as a baseline analysis of forest structure dynamics for complete Germany. The complementary information over time allows to characterize different post-disturbance structures in forests having significant influence on forest regeneration and future resilience, e.g., to differentiate salvage logging and standing deadwood [18,83–85]. Recent efforts of the GEDI science team on extending the GEDI mission (end of data acquisition in March 2023) would greatly support the analysis on forest dynamics such as recovery after disturbance or the global mapping of AGBD [86–88]. Furthermore, the multi-temporal analysis of forest structure as presented in the present and other studies [36,71], specifically modeling historical conditions of forest structure (e.g., based on Landsat since the 1980s) would

improve the understanding of long-term carbon balance dynamics in the context of land use history. In addition, the derivation of complementary forest structure characteristics also supports the analysis of biodiversity since recent popular remote sensing concepts (spectral diversity [89–92]) are primarily based on multispectral information [93].

## 5. Conclusions

The present study demonstrates the derivation of consistent forest structure information for forests in Germany, thus allowing for a comprehensive characterization of canopy height, total canopy cover and AGBD at different spatial and temporal scales. On the one hand, accurate overall characteristics of forest structure in Germany were assessed in high spatial resolution (10 m) and on the other hand, large-scale dynamics of forest disturbance as a consequence of the recent past drought years (2018, 2019, 2020, 2022) and several significant storm events were monitored. The following bullet points summarize the main findings:

- There is a decline in mean canopy height in Germany from 2017 (about 22.5 m) to 2022 (about 20 m). A growing proportion of low canopy height areas is indicated by the multi-temporal modeling approach: In recent years about 25% of German forest canopy heights are in a range from 11 to 18 m (2022) opposing to a range of 13 to 20 m in 2017. The highest losses in canopy height are occurring in Saxony-Anhalt (mean difference in canopy height comparing 2022 to 2017:  $-4.8$  m) and North Rhine-Westphalia ( $-3.2$  m).
- Mean total canopy cover values at the country level from 2017 to 2022 present rather stable values within a range from 55 to 60%. Nevertheless, a growing number of areas with open canopy covers is quantified by an increased quartile group one spanning from the minimum to the first quartile (about 20 to 50%) in 2021 and 2022 compared to 2017 (about 35 to 50%). Mean difference statistics of total canopy cover highlight strong losses (lower than  $-5\%$ ) in Saxony-Anhalt and Brandenburg opposing to gains in cover density in Rhineland-Palatinate and Saarland (greater than  $7\%$ ).
- The quantitative analysis of AGBD presents a steady decline in mean AGBD in Germany from 2017 (about 200 Mg/ha) to 2022 (about 165 Mg/ha). Saxony-Anhalt, North Rhine-Westphalia, Mecklenburg Western Pomerania, Thuringia and Brandenburg are the federal states with strongest losses indicated by a mean difference in AGBD between 2022 and 2017 of lower than  $-30$  Mg/ha.
- Difference maps of forest structure for the Harz region highlight the dominance of strong negative changes in coniferous stands which are spatially corresponding to the canopy cover loss areas mapped by Thonfeld et al., 2022 [29]. Furthermore, there are asynchronous temporal dynamics in canopy height, cover density and AGBD for the Harz region enabling a more detailed understanding of post-disturbance conditions.

To conclude, the wall-to-wall coverage of six years of forest structure information for Germany not only allows for an improved understanding of future forest resilience towards disturbance in the context of climate change, but also supports the generation of products related to biodiversity at multiple scales (alpha, beta, gamma diversity).

**Author Contributions:** Conceptualization, P.K., F.T. and C.K.; methodology, P.K.; software, P.K.; validation, P.K.; formal analysis, P.K.; writing—original draft preparation, P.K.; writing—review and editing, P.K., F.T., U.G. and C.K.; visualization, P.K.; supervision, U.G. and C.K.; project administration, C.K.; funding acquisition, C.K. All authors have read and agreed to the published version of the manuscript.

**Funding:** This research has been supported by the DFG (Deutsche Forschungsgemeinschaft) within the framework of the Research Unit BETA-FOR (Enhancing the structural diversity between patches for improving multidiversity and multifunctionality in production forests) (grant no. FOR 5375/1, project number 459717468).

**Data Availability Statement:** The multi-annual forest structure maps are available from the corresponding author upon reasonable request.

**Conflicts of Interest:** The authors declare no conflict of interest.

## Appendix A

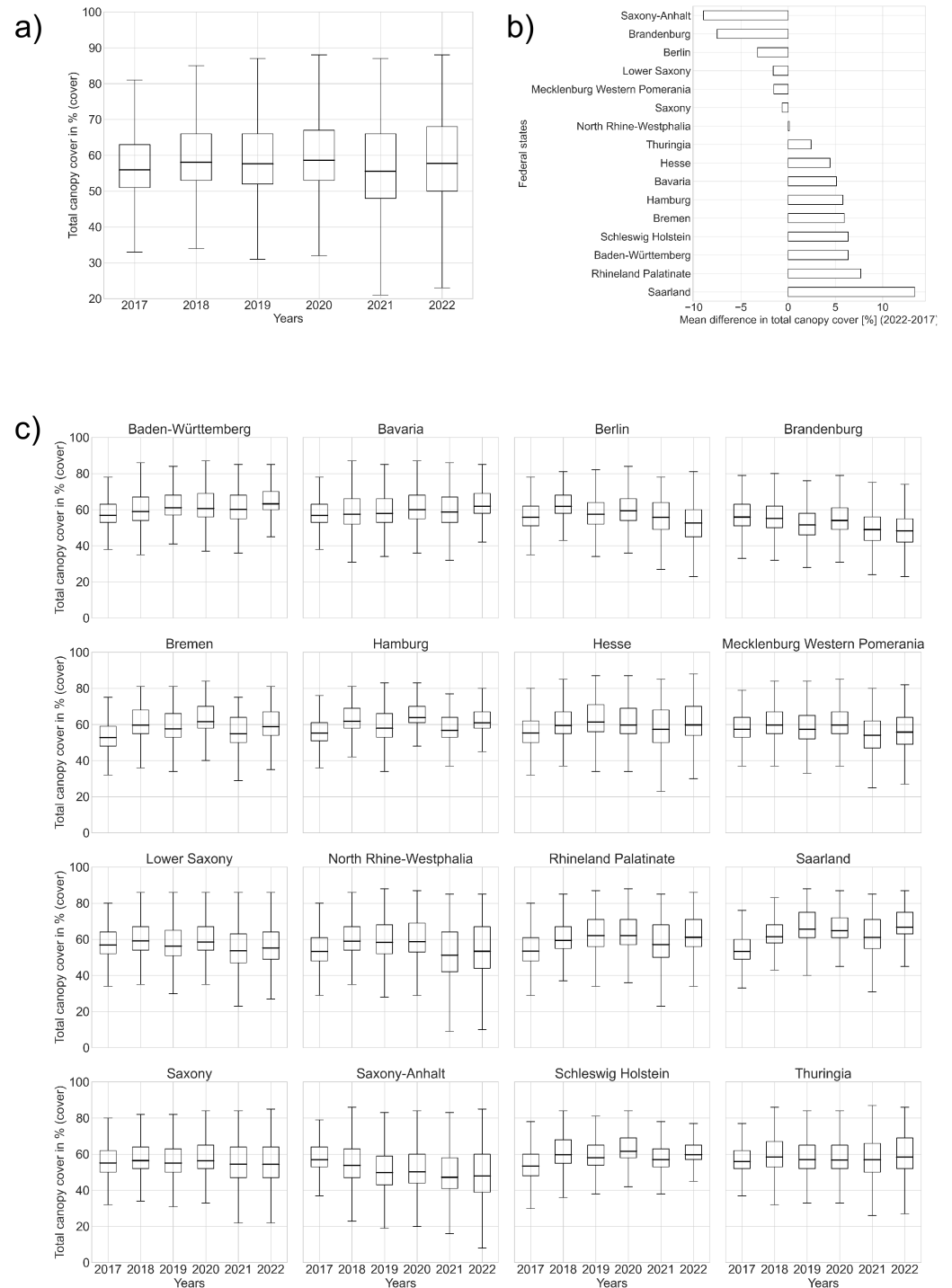


**Figure A1.** Quantitative statistics of total canopy cover in forested areas of Germany: Overall dynamics in total canopy cover in Germany (a), mean difference in total canopy cover (2022-2017) among federal states (b), multi-temporal change in total canopy cover grouped by federal states (c). The statistics are based on predicted pixel estimates depicting mean values as horizontal line in the boxplots. General dynamics of forest structure are assessed; absolute values should be interpreted in the context of model uncertainty.

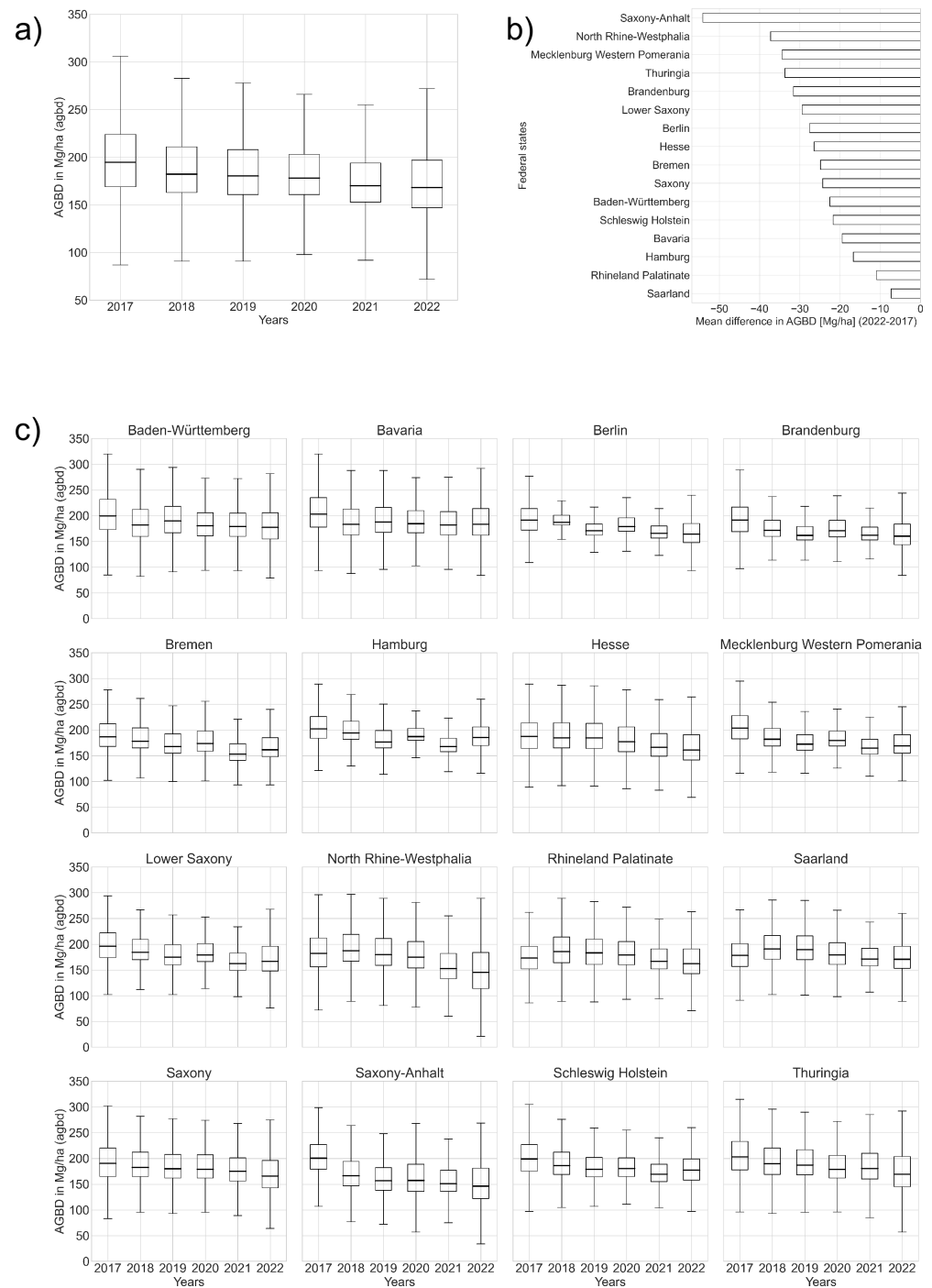


**Figure A2.** Quantitative statistics of AGBD in forested areas of Germany: Overall dynamics in AGBD in Germany (a), mean difference in AGBD (2022–2017) among federal states (b), multi-temporal change in AGBD grouped by federal states (c). The statistics are based on predicted pixel estimates depicting mean values as horizontal line in the boxplots. General dynamics of forest structure are assessed; absolute values should be interpreted in the context of model uncertainty.

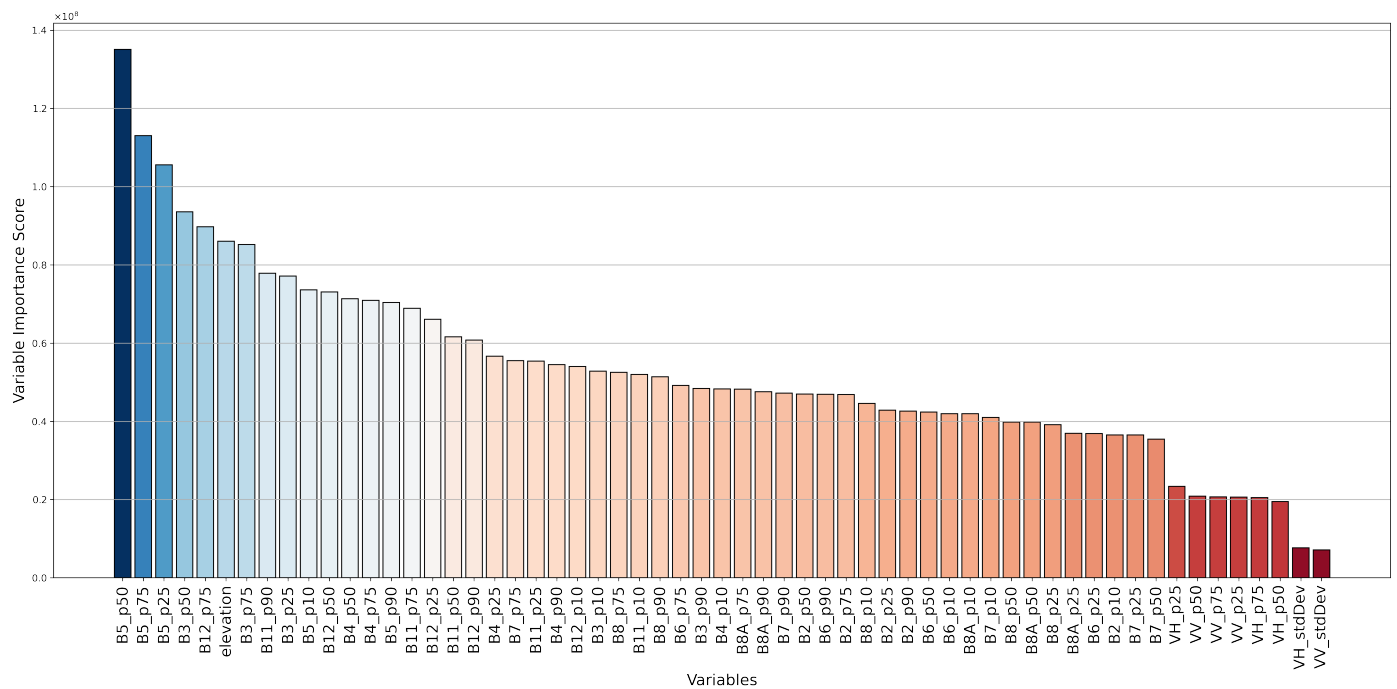


**Figure A3.** Variable importance scores of the 2022 canopy height model (rh\_95). Abbreviations of sensors: Sentinel-1 (VV = vertical-vertical polarization, VH = vertical-horizontal polarization), Sentinel-2 (B\*, e.g., B5, [https://developers.google.com/earth-engine/datasets/catalog/COPERNICUS\\_S2\\_SR\\_HARMONIZED](https://developers.google.com/earth-engine/datasets/catalog/COPERNICUS_S2_SR_HARMONIZED), accessed on 12 February 2023). SRTM (elevation). Temporal statistics are abbreviated as follows: “p50” (50th percentile), “stdDev” (standard deviation).

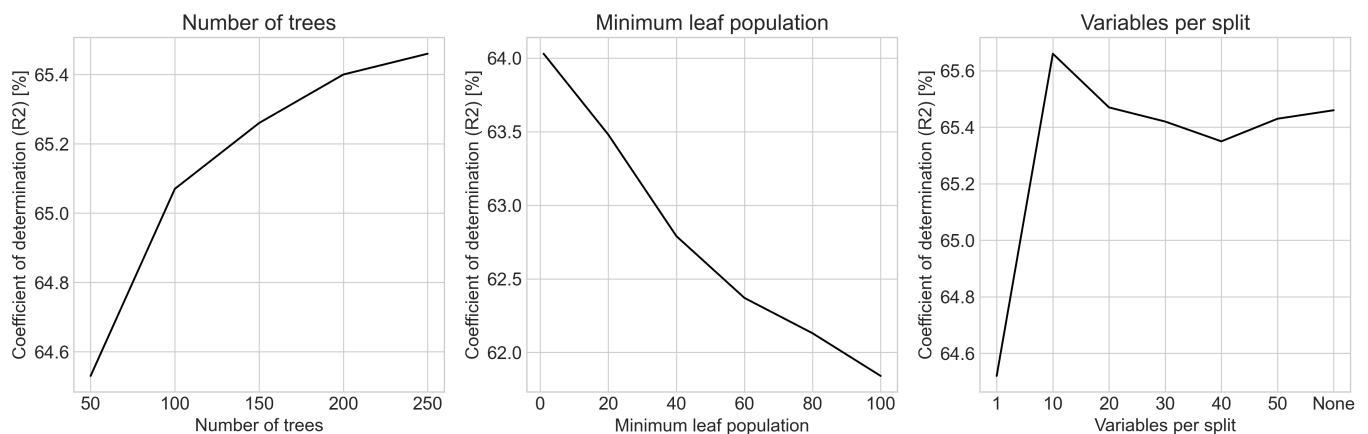


**Figure A4.** Sensitivity analysis for the 2022 canopy height model highlighting increased model accuracy when specifying a high number of trees, low minimum leaf population and a rather low number of variables per split.

## References

1. Buras, A.; Rammig, A.; Zang, C.S. Quantifying impacts of the 2018 drought on European ecosystems in comparison to 2003. *Biogeosciences* **2020**, *17*, 1655–1672. [\[CrossRef\]](#)
2. Rakovec, O.; Samaniego, L.; Hari, V.; Markonis, Y.; Moravec, V.; Thober, S.; Hanel, M.; Kumar, R. The 2018–2020 Multi-year drought sets a new benchmark in Europe. *Earth's Future* **2022**, *10*, e2021EF002394. [\[CrossRef\]](#)
3. Senf, C.; Buras, A.; Zang, C.S.; Rammig, A.; Seidl, R. Excess forest mortality is consistently linked to drought across Europe. *Nat. Commun.* **2020**, *11*, 6200. [\[CrossRef\]](#)

4. Schuldts, B.; Buras, A.; Arend, M.; Vitasse, Y.; Beierkuhnlein, C.; Damm, A.; Gharun, M.; Grams, T.E.; Hauck, M.; Hajek, P.; et al. A first assessment of the impact of the extreme 2018 summer drought on Central European forests. *Basic Appl. Ecol.* **2020**, *45*, 86–103. [CrossRef]
5. Statistical office of the European Union (Eurostat). Share of Timber Removals to Net Increment in EU Forests. 2020. Available online: [https://ec.europa.eu/eurostat/statistics-explained/index.php?title=File:Figure\\_3\\_Share\\_of\\_timber\\_removals\\_to\\_net\\_increment\\_in\\_EU\\_forests,\\_2020\\_\(%25\).png](https://ec.europa.eu/eurostat/statistics-explained/index.php?title=File:Figure_3_Share_of_timber_removals_to_net_increment_in_EU_forests,_2020_(%25).png) (accessed on 26 January 2023).
6. Federal Ministry of Food and Agriculture (BMEL). Waldbericht der Bundesregierung 2021. Available online: [https://www.bmel.de/SharedDocs/Downloads/DE/Broschueren/waldbericht2021.pdf?\\_\\_blob=publicationFile&v=11](https://www.bmel.de/SharedDocs/Downloads/DE/Broschueren/waldbericht2021.pdf?__blob=publicationFile&v=11) (accessed on 25 January 2023).
7. Statistisches Bundesamt (Destatis). Flächengröße des Waldes nach Bundesländern. Available online: <https://www.destatis.de/DE/Themen/Branchen-Unternehmen/Landwirtschaft-Forstwirtschaft-Fischerei/Wald-Holz/Tabellen/waldflaeche-bundeslaender.html> (accessed on 25 January 2023).
8. Statistisches Bundesamt (Destatis). Structural Survey of Forestry Holdings: Forest Area by Types of Forest Ownership. Available online: <https://www.destatis.de/EN/Themes/Economic-Sectors-Enterprises/Agriculture-Forestry-Fisheries/Forestry-Wood/Tables/structural-survey-of-forestry-holdings-forest-area-by-types-of-forest-ownership.html> (accessed on 25 January 2023).
9. Statistical office of the European Union (Eurostat). Employment in Forestry and Logging, 2000 and 2020. Available online: [https://ec.europa.eu/eurostat/statistics-explained/index.php?title=File:Table\\_2\\_Employment\\_in\\_forestry\\_and\\_logging,\\_2000\\_and\\_2020.png](https://ec.europa.eu/eurostat/statistics-explained/index.php?title=File:Table_2_Employment_in_forestry_and_logging,_2000_and_2020.png) (accessed on 26 January 2023).
10. Statistisches Bundesamt (Destatis). Exports of Raw Timber up 42.6% in 2020. Available online: [https://www.destatis.de/EN/Press/2021/05/PE21\\_N031\\_51.html](https://www.destatis.de/EN/Press/2021/05/PE21_N031_51.html) (accessed on 25 January 2023).
11. Statistisches Bundesamt (Destatis). 2008 to 2018: Sawmills Increase Their Turnover and Now Earn One in Three Euros Abroad. Available online: [https://www.destatis.de/EN/Press/2019/09/PE19\\_377\\_412.html](https://www.destatis.de/EN/Press/2019/09/PE19_377_412.html) (accessed on 25 January 2023).
12. European Environment Agency. Dominant Leaf Type 2018. 2020. Available online: <https://land.copernicus.eu/pan-european/high-resolution-layers/forests/dominant-leaf-type/status-maps/dominant-leaf-type-2018> (accessed on 3 February 2023).
13. Johann Heinrich von Thünen Institute (Federal Research Institute for Rural Areas, Forestry and Fisheries)—Institute of Forest Ecosystems. Ergebnisse der Bundesweiten Waldzustandserhebung. Available online: <https://wo-apps.thuenen.de/apps/wze/> (accessed on 12 January 2023).
14. Statistisches Bundesamt (Destatis). Impact of Extreme wind and Weather Conditions on the Forests. Available online: [https://www.destatis.de/EN/Press/2020/02/PE20\\_N006\\_413.html](https://www.destatis.de/EN/Press/2020/02/PE20_N006_413.html) (accessed on 25 January 2023).
15. Statistisches Bundesamt (Destatis). Forest Damage: Logging of Timber Damaged by Insect Infestation Grew More than Tenfold within Five Years. Available online: [https://www.destatis.de/EN/Press/2021/08/PE21\\_N050\\_41.html](https://www.destatis.de/EN/Press/2021/08/PE21_N050_41.html) (accessed on 25 January 2023).
16. Statistisches Bundesamt (Destatis). Total Timber Cutting by Cutting Cause and Forest Ownership Types. Available online: <https://www.destatis.de/EN/Themes/Economic-Sectors-Enterprises/Agriculture-Forestry-Fisheries/Forestry-Wood/Tables/timber-cutting-causes.html> (accessed on 25 January 2023).
17. Federal Ministry of Food and Agriculture (BMEL). Ergebnisse der Waldzustandserhebung 2021. Available online: [https://www.bmel.de/SharedDocs/Downloads/DE/Broschueren/ergebnisse-waldzustandserhebung-2021.pdf?\\_\\_blob=publicationFile&v=10](https://www.bmel.de/SharedDocs/Downloads/DE/Broschueren/ergebnisse-waldzustandserhebung-2021.pdf?__blob=publicationFile&v=10) (accessed on 25 January 2023).
18. Thorn, S.; Bässler, C.; Brandl, R.; Burton, P.J.; Cahall, R.; Campbell, J.L.; Castro, J.; Choi, C.Y.; Cobb, T.; Donato, D.C.; et al. Impacts of salvage logging on biodiversity: A meta-analysis. *J. Appl. Ecol.* **2018**, *55*, 279–289. [CrossRef]
19. Holzwarth, S.; Thonfeld, F.; Abdullahi, S.; Asam, S.; Da Ponte Canova, E.; Gessner, U.; Huth, J.; Kraus, T.; Leutner, B.; Kuenzer, C. Earth observation based monitoring of forests in Germany: A review. *Remote Sens.* **2020**, *12*, 3570. [CrossRef]
20. Wellbrock, N.; Bolte, A. *Status and Dynamics of Forests in Germany: Results of the National Forest Monitoring*; Springer: Berlin/Heidelberg, Germany, 2019.
21. Jetz, W.; Cavender-Bares, J.; Pavlick, R.; Schimel, D.; Davis, F.W.; Asner, G.P.; Guralnick, R.; Kattge, J.; Latimer, A.M.; Moorcroft, P.; et al. Monitoring plant functional diversity from space. *Nat. Plants* **2016**, *2*, 1–5.
22. Randin, C.F.; Ashcroft, M.B.; Bolliger, J.; Cavender-Bares, J.; Coops, N.C.; Dullinger, S.; Dirnböck, T.; Eckert, S.; Ellis, E.; Fernández, N.; et al. Monitoring biodiversity in the Anthropocene using remote sensing in species distribution models. *Remote Sens. Environ.* **2020**, *239*, 111626. [CrossRef]
23. Hansen, M.C.; Potapov, P.V.; Moore, R.; Hancher, M.; Turubanova, S.A.; Tyukavina, A.; Thau, D.; Stehman, S.V.; Goetz, S.J.; Loveland, T.R.; et al. High-Resolution Global Maps of 21st-Century Forest Cover Change. *Science* **2013**, *342*, 850–853. [CrossRef] [PubMed]
24. Hansen, M.; Egorov, A.; Potapov, P.; Stehman, S.; Tyukavina, A.; Turubanova, S.; Roy, D.; Goetz, S.; Loveland, T.; Ju, J.; et al. Monitoring conterminous United States (CONUS) land cover change with Web-Enabled Landsat Data (WELD). *Remote Sens. Environ.* **2014**, *140*, 466–484. [CrossRef]
25. Montzka, C.; Bayat, B.; Tewes, A.; Mengen, D.; Vereecken, H. Sentinel-2 analysis of spruce crown transparency levels and their environmental drivers after summer drought in the Northern Eifel (Germany). *Front. For. Glob. Chang.* **2021**, *4*, 667151. [CrossRef]
26. Philipp, M.; Wegmann, M.; Kübert-Flock, C. Quantifying the response of German forests to drought events via Satellite imagery. *Remote Sens.* **2021**, *13*, 1845. [CrossRef]



27. European Environment Agency. *Forest Type 2015*; European Environment Agency: Copenhagen, Denmark, 2017.
28. European Environment Agency. *Tree Cover Density 2018*; European Environment Agency: Copenhagen, Denmark, 2020.
29. Thonfeld, F.; Gessner, U.; Holzwarth, S.; Kriese, J.; Da Ponte, E.; Huth, J.; Kuenzer, C. A First Assessment of Canopy Cover Loss in Germany's Forests after the 2018–2020 Drought Years. *Remote Sens.* **2022**, *14*, 562. [[CrossRef](#)]
30. Welle, T.; Aschenbrenner, L.; Kuonath, K.; Kirmaier, S.; Franke, J. Mapping Dominant Tree Species of German Forests. *Remote Sens.* **2022**, *14*, 3330. [[CrossRef](#)]
31. Bruening, J.M.; Fischer, R.; Bohn, F.J.; Armston, J.; Armstrong, A.H.; Knapp, N.; Tang, H.; Huth, A.; Dubayah, R. Challenges to aboveground biomass prediction from waveform lidar. *Environ. Res. Lett.* **2021**, *16*, 125013. [[CrossRef](#)]
32. Fischer, R.; Knapp, N.; Bohn, F.; Shugart, H.H.; Huth, A. The relevance of forest structure for biomass and productivity in temperate forests: New perspectives for remote sensing. *Surv. Geophys.* **2019**, *40*, 709–734. [[CrossRef](#)]
33. Marselis, S.M.; Abernethy, K.; Alonso, A.; Armston, J.; Baker, T.R.; Bastin, J.F.; Bogaert, J.; Boyd, D.S.; Boeckx, P.; Burslem, D.F.; et al. Evaluating the potential of full-waveform lidar for mapping pan-tropical tree species richness. *Glob. Ecol. Biogeogr.* **2020**, *29*, 1799–1816. [[CrossRef](#)]
34. Marselis, S.M.; Keil, P.; Chase, J.M.; Dubayah, R. The use of GEDI canopy structure for explaining variation in tree species richness in natural forests. *Environ. Res. Lett.* **2022**, *17*, 045003. [[CrossRef](#)]
35. Schneider, F.D.; Ferraz, A.; Hancock, S.; Duncanson, L.I.; Dubayah, R.O.; Pavlick, R.P.; Schimel, D.S. Towards mapping the diversity of canopy structure from space with GEDI. *Environ. Res. Lett.* **2020**, *15*, 115006. [[CrossRef](#)]
36. Potapov, P.; Li, X.; Hernandez-Serna, A.; Tyukavina, A.; Hansen, M.C.; Kommareddy, A.; Pickens, A.; Turubanova, S.; Tang, H.; Silva, C.E.; et al. Mapping global forest canopy height through integration of GEDI and Landsat data. *Remote Sens. Environ.* **2021**, *253*, 112165. [[CrossRef](#)]
37. Lang, N.; Kalischek, N.; Armston, J.; Schindler, K.; Dubayah, R.; Wegner, J.D. Global canopy height regression and uncertainty estimation from GEDI LIDAR waveforms with deep ensembles. *Remote Sens. Environ.* **2022**, *268*, 112760. [[CrossRef](#)]
38. Dubayah, R.; Blair, J.B.; Goetz, S.; Fatoyinbo, L.; Hansen, M.; Healey, S.; Hofton, M.; Hurtt, G.; Kellner, J.; Luthcke, S.; et al. The Global Ecosystem Dynamics Investigation: High-resolution laser ranging of the Earth's forests and topography. *Sci. Remote Sens.* **2020**, *1*, 100002. [[CrossRef](#)]
39. Duncanson, L.; Neuenschwander, A.; Hancock, S.; Thomas, N.; Fatoyinbo, T.; Simard, M.; Silva, C.A.; Armston, J.; Luthcke, S.B.; Hofton, M.; et al. Biomass estimation from simulated GEDI, ICESat-2 and NISAR across environmental gradients in Sonoma County, California. *Remote Sens. Environ.* **2020**, *242*, 111779. [[CrossRef](#)]
40. Skidmore, A.K.; Coops, N.C.; Neinavaz, E.; Ali, A.; Schaeppman, M.E.; Paganini, M.; Kissling, W.D.; Vihervaara, P.; Darvishzadeh, R.; Feilhauer, H.; et al. Priority list of biodiversity metrics to observe from space. *Nat. Ecol. Evol.* **2021**, *5*, 896–906. [[CrossRef](#)] [[PubMed](#)]
41. Abdullahi, S.; Schardt, M.; Pretzsch, H. An unsupervised two-stage clustering approach for forest structure classification based on X-band InSAR data—A case study in complex temperate forest stands. *Int. J. Appl. Earth Obs. Geoinf.* **2017**, *57*, 36–48. [[CrossRef](#)]
42. Cazcarra-Bes, V.; Pardini, M.; Papathanassiou, K. Definition of tomographic SAR configurations for forest structure applications at L-band. *IEEE Geosci. Remote Sens. Lett.* **2020**, *19*, 1–5. [[CrossRef](#)]
43. Drag, L.; Burner, R.C.; Stephan, J.G.; Birkemoe, T.; Doerfler, I.; Gossner, M.M.; Magdon, P.; Ovaskainen, O.; Potterf, M.; Schall, P.; et al. High-resolution 3D forest structure explains ecomorphological trait variation in assemblages of saproxylic beetles. *Funct. Ecol.* **2022**, *37*, 150–161. [[CrossRef](#)]
44. Pardini, M.; Cazcarra-Bes, V.; Papathanassiou, K.P. TomoSAR mapping of 3D forest structure: Contributions of L-band configurations. *Remote Sens.* **2021**, *13*, 2255. [[CrossRef](#)]
45. Schlund, M.; Magdon, P.; Eaton, B.; Aumann, C.; Erasmi, S. Canopy height estimation with TanDEM-X in temperate and boreal forests. *Int. J. Appl. Earth Obs. Geoinf.* **2019**, *82*, 101904. [[CrossRef](#)]
46. Senf, C.; Mori, A.S.; Müller, J.; Seidl, R. The response of canopy height diversity to natural disturbances in two temperate forest landscapes. *Landsc. Ecol.* **2020**, *35*, 2101–2112. [[CrossRef](#)]
47. Tello, M.; Cazcarra-Bes, V.; Pardini, M.; Papathanassiou, K. Forest structure characterization from SAR tomography at L-band. *IEEE J. Sel. Top. Appl. Earth Obs. Remote Sens.* **2018**, *11*, 3402–3414. [[CrossRef](#)]
48. Wernicke, J.; Seltmann, C.T.; Wenzel, R.; Becker, C.; Körner, M. Forest canopy stratification based on fused, imbalanced and collinear LiDAR and Sentinel-2 metrics. *Remote Sens. Environ.* **2022**, *279*, 113134. [[CrossRef](#)]
49. Pucher, C.; Neumann, M.; Hasenauer, H. An Improved Forest Structure Data Set for Europe. *Remote Sens.* **2022**, *14*, 395. [[CrossRef](#)]
50. Kacic, P.; Hirner, A.; Da Ponte, E. Fusing Sentinel-1 and-2 to Model GEDI-Derived Vegetation Structure Characteristics in GEE for the Paraguayan Chaco. *Remote Sens.* **2021**, *13*, 5105. [[CrossRef](#)]
51. Mullissa, A.; Vollrath, A.; Odongo-Braun, C.; Slagter, B.; Balling, J.; Gou, Y.; Gorelick, N.; Reiche, J. Sentinel-1 SAR Backscatter Analysis Ready Data Preparation in Google Earth Engine. *Remote Sens.* **2021**, *13*, 1954. [[CrossRef](#)]
52. Louis, J.; Debaecker, V.; Pflug, B.; Main-Knorn, M.; Bieniarz, J.; Mueller-Wilm, U.; Cadau, E.; Gascon, F. Sentinel-2 Sen2Cor: L2A processor for users. In Proceedings of the Proceedings Living Planet Symposium 2016, Spacebooks Online, 9 May 2016; pp. 1–8.
53. Main-Knorn, M.; Pflug, B.; Louis, J.; Debaecker, V.; Müller-Wilm, U.; Gascon, F. Sen2Cor for sentinel-2. In *Proceedings of the Image and Signal Processing for Remote Sensing XXIII*; SPIE: Bellingham, DC, USA, 2017; Volume 10427, pp. 37–48.
54. Gorelick, N.; Hancher, M.; Dixon, M.; Ilyushchenko, S.; Thau, D.; Moore, R. Google Earth Engine: Planetary-scale geospatial analysis for everyone. *Remote Sens. Environ.* **2017**, *202*, 18–27. [[CrossRef](#)]

55. Dubayah, R.; Hofton, M.; Blair, J.; Armston, J.; Tang, H.; Luthcke, S. GEDI L2A Elevation and Height Metrics Data Global Footprint Level V002. 2021. Available online: [https://lpdaac.usgs.gov/products/gedi02\\_av002/](https://lpdaac.usgs.gov/products/gedi02_av002/) (accessed on 11 October 2022).
56. Dubayah, R.; Tang, H.; Armston, J.; Luthcke, S.; Hofton, M.; Blair, J. GEDI L2B Canopy Cover and Vertical Profile Metrics Data Global Footprint Level V002. 2021. Available online: <https://lpdaac.usgs.gov/news/release-of-gedi-v2-data-for-february-through-june-2021/> (accessed on 11 October 2022). [CrossRef]
57. Dubayah, R. GEDI L2B Description Update Release 2. Canopy Cover and Vertical Profile Metrics Data Global Footprint Level 2021. Available online: [https://lpdaac.usgs.gov/products/gedi02\\_bv001/](https://lpdaac.usgs.gov/products/gedi02_bv001/) (accessed on 11 October 2022).
58. Dubayah, R.; Armston, J.; Kellner, J.; Duncanson, L.; Healey, S.; Patterson, P.; Hancock, S.; Tang, H.; Bruening, J.; Hofton, M.; et al. *GEDI L4A Footprint Level Aboveground Biomass Density*; Version 2.1.; ORNL DAAC: Oak Ridge, TN, USA, 2022.
59. Tang, H.; Armston, J. Algorithm Theoretical Basis Document (ATBD) for GEDI L2B Footprint Canopy Cover and Vertical Profile Metrics. 2020. Available online: [https://lpdaac.usgs.gov/documents/588/GEDI\\_FCCVPM\\_ATBD\\_v1.0.pdf](https://lpdaac.usgs.gov/documents/588/GEDI_FCCVPM_ATBD_v1.0.pdf) (accessed on 11 October 2022).
60. Kellner, J.R.; Armston, J.; Duncanson, L. Algorithm theoretical basis document for GEDI footprint aboveground biomass density (1.0). *Earth Space Sci.* **2021**, e2022EA002516.
61. Hoffrén, R.; Lamelas, M.T.; de la Riva, J.; Domingo, D.; Montealegre, A.L.; García-Martín, A.; Revilla, S. Assessing GEDI-NASA system for forest fuels classification using machine learning techniques. *Int. J. Appl. Earth Obs. Geoinf.* **2023**, *116*, 103175. [CrossRef]
62. Franklin, S.E.; Ahmed, O.S.; Wulder, M.A.; White, J.C.; Hermosilla, T.; Coops, N.C. Large Area Mapping of Annual Land Cover Dynamics Using Multitemporal Change Detection and Classification of Landsat Time Series Data. *Can. J. Remote Sens.* **2015**, *41*, 293–314. [CrossRef]
63. Müller, H.; Griffiths, P.; Hostert, P. Long-term deforestation dynamics in the Brazilian Amazon—Uncovering historic frontier development along the Cuiabá–Santarém highway. *Int. J. Appl. Earth Obs. Geoinf.* **2016**, *44*, 61–69. [CrossRef]
64. Zanaga, D.; Van De Kerchove, R.; De Keersmaecker, W.; Souverijns, N.; Brockmann, C.; Quast, R.; Wevers, J.; Grosu, A.; Paccini, A.; Vergnaud, S.; et al. ESA WorldCover 10 m 2020 V100. 2021. Available online: [https://developers.google.com/earth-engine/datasets/catalog/ESA\\_WorldCover\\_v100](https://developers.google.com/earth-engine/datasets/catalog/ESA_WorldCover_v100) (accessed on 4 December 2022).
65. Breiman, L. Bagging predictors. *Mach. Learn.* **1996**, *24*, 123–140. [CrossRef]
66. Breiman, L. Random forests. *Mach. Learn.* **2001**, *45*, 5–32. [CrossRef]
67. Belgiu, M.; Drăguț, L. Random forest in remote sensing: A review of applications and future directions. *Isprs J. Photogramm. Remote Sens.* **2016**, *114*, 24–31. [CrossRef]
68. Pal, M. Random forest classifier for remote sensing classification. *Int. J. Remote Sens.* **2005**, *26*, 217–222. [CrossRef]
69. Sothe, C.; Gonsamo, A.; Lourenço, R.B.; Kurz, W.A.; Snider, J. Spatially Continuous Mapping of Forest Canopy Height in Canada by Combining GEDI and ICESat-2 with PALSAR and Sentinel. *Remote Sens.* **2022**, *14*, 5158. [CrossRef]
70. Rishmawi, K.; Huang, C.; Zhan, X. Monitoring Key Forest Structure Attributes across the Conterminous United States by Integrating GEDI LiDAR Measurements and VIIRS Data. *Remote Sens.* **2021**, *13*, 442. [CrossRef]
71. Rishmawi, K.; Huang, C.; Schleeweis, K.; Zhan, X. Integration of VIIRS Observations with GEDI-Lidar Measurements to Monitor Forest Structure Dynamics from 2013 to 2020 across the Conterminous United States. *Remote Sens.* **2022**, *14*, 2320. [CrossRef]
72. Bundesamt für Kartographie und Geodäsie. GeoBasis-DE/BKG Digitales Landschaftsmodell 1:250,000 (DLM250). 2020. Available online: <https://gdz.bkg.bund.de/index.php/default/digitales-landschaftsmodell-1-250-000-ebenen-dlm250-ebenen.html> (accessed on 28 December 2022).
73. Lang, N.; Schindler, K.; Wegner, J.D. High carbon stock mapping at large scale with optical satellite imagery and spaceborne LIDAR. 2021. Available online: <http://xxx.lanl.gov/abs/2107.07431> (accessed on 5 January 2023).
74. Verheyen, R. *Rechtliche Optionen für den Dannenröder Wald: Rodungsstopp, Ergänzungsverfahren-Ist das Wirklich unmöglich?* Greenpeace eV Hamburg: Hamburg, Germany, 2020.
75. Jung, C.; Schindler, D. Historical winter storm atlas for Germany (GeWiSA). *Atmosphere* **2019**, *10*, 387. [CrossRef]
76. Adam, M.; Urbazaev, M.; Dubois, C.; Schnullius, C. Accuracy Assessment of GEDI Terrain Elevation and Canopy Height Estimates in European Temperate Forests: Influence of Environmental and Acquisition Parameters. *Remote Sens.* **2020**, *12*, 3948. [CrossRef]
77. Roy, D.P.; Kashongwe, H.B.; Armston, J. The impact of geolocation uncertainty on GEDI tropical forest canopy height estimation and change monitoring. *Sci. Remote Sens.* **2021**, *4*, 100024. [CrossRef]
78. Wang, C.; Elmore, A.J.; Numata, I.; Cochrane, M.A.; Shaogang, L.; Huang, J.; Zhao, Y.; Li, Y. Factors affecting relative height and ground elevation estimations of GEDI among forest types across the conterminous USA. *Gisci. Remote Sens.* **2022**, *59*, 975–999. [CrossRef]
79. Hirschmugl, M.; Lippl, F.; Sobe, C. Assessing the Vertical Structure of Forests Using Airborne and Spaceborne LiDAR Data in the Austrian Alps. *Remote Sens.* **2023**, *15*, 664. [CrossRef]
80. Arekhi, M.; Goksel, C.; Balik Sanli, F.; Senel, G. Comparative evaluation of the spectral and spatial consistency of Sentinel-2 and Landsat-8 OLI data for Igneada longos forest. *Isprs Int. J.-Geo-Inf.* **2019**, *8*, 56. [CrossRef]
81. Kotttek, M.; Grieser, J.; Beck, C.; Rudolf, B.; Rubel, F. World map of the Köppen–Geiger Climate Classification Updated. 2006. Available online: [https://www.schweizerbart.de/papers/metz/detail/15/55034/World\\_Map\\_of\\_the\\_Koppen\\_Geiger\\_climate\\_classificat?af=crossref](https://www.schweizerbart.de/papers/metz/detail/15/55034/World_Map_of_the_Koppen_Geiger_climate_classificat?af=crossref) (accessed on 20 January 2023).

82. Peel, M.C.; Finlayson, B.L.; McMahon, T.A. Updated world map of the Köppen-Geiger climate classification. *Hydrol. Earth Syst. Sci.* **2007**, *11*, 1633–1644. [[CrossRef](#)]
83. Hlásny, T.; Krokene, P.; Liebhold, A.; Montagné-Huck, C.; Müller, J.; Qin, H.; Raffa, K.; Schelhaas, M.; Seidl, R.; Svoboda, M.; et al. *Living with Bark Beetles: Impacts, Outlook and Management Options*; Number 8; European Forest Institute: Joensuu, Finland, 2019.
84. Hlásny, T.; König, L.; Krokene, P.; Lindner, M.; Montagné-Huck, C.; Müller, J.; Qin, H.; Raffa, K.F.; Schelhaas, M.J.; Svoboda, M.; et al. Bark beetle outbreaks in Europe: State of knowledge and ways forward for management. *Curr. For. Rep.* **2021**, *7*, 138–165. [[CrossRef](#)]
85. Thorn, S.; Bässler, C.; Svoboda, M.; Müller, J. Effects of natural disturbances and salvage logging on biodiversity—Lessons from the Bohemian Forest. *For. Ecol. Manag.* **2017**, *388*, 113–119. [[CrossRef](#)]
86. Duncanson, L.; Kellner, J.R.; Armston, J.; Dubayah, R.; Minor, D.M.; Hancock, S.; Healey, S.P.; Patterson, P.L.; Saarela, S.; Marselis, S.; et al. Aboveground biomass density models for NASA’s Global Ecosystem Dynamics Investigation (GEDI) lidar mission. *Remote Sens. Environ.* **2022**, *270*, 112845. [[CrossRef](#)]
87. Dubayah, R.; Armston, J.; Healey, S.P.; Bruening, J.M.; Patterson, P.L.; Kellner, J.R.; Duncanson, L.; Saarela, S.; Ståhl, G.; Yang, Z.; et al. GEDI launches a new era of biomass inference from space. *Environ. Res. Lett.* **2022**, *17*, 095001. [[CrossRef](#)]
88. GEDI Ecosystem Lidar. GEDI could Get Extension under New Proposal. Available online: <https://gedi.umd.edu/gedi-could-get-extension-under-new-proposal/> (accessed on 27 January 2023).
89. Rocchini, D.; Salvatori, N.; Beierkuhnlein, C.; Chiarucci, A.; De Boissieu, F.; Förster, M.; Garzon-Lopez, C.X.; Gillespie, T.W.; Haufler, H.C.; He, K.S.; et al. From local spectral species to global spectral communities: A benchmark for ecosystem diversity estimate by remote sensing. *Ecol. Inform.* **2021**, *61*, 101195. [[CrossRef](#)]
90. Rocchini, D.; Torresani, M.; Beierkuhnlein, C.; Feoli, E.; Foody, G.M.; Lenoir, J.; Malavasi, M.; Moudry, V.; Šimová, P.; Ricotta, C. Double down on remote sensing for biodiversity estimation: a biological mindset. *Community Ecol.* **2022**, *23*, 267–276. [[CrossRef](#)]
91. Rocchini, D.; Santos, M.J.; Ustin, S.L.; Féret, J.B.; Asner, G.P.; Beierkuhnlein, C.; Dalponte, M.; Feilhauer, H.; Foody, G.M.; Geller, G.N.; et al. The spectral species concept in living color. *J. Geophys. Res. Biogeosci.* **2022**, *127*, e2022JG007026. [[CrossRef](#)] [[PubMed](#)]
92. Wang, R.; Gamon, J.A. Remote sensing of terrestrial plant biodiversity. *Remote Sens. Environ.* **2019**, *231*, 111218. [[CrossRef](#)]
93. Kacic, P.; Kuenzer, C. Forest Biodiversity Monitoring Based on Remotely Sensed Spectral Diversity—A Review. *Remote Sens.* **2022**, *14*, 5363. [[CrossRef](#)]

**Disclaimer/Publisher’s Note:** The statements, opinions and data contained in all publications are solely those of the individual author(s) and contributor(s) and not of MDPI and/or the editor(s). MDPI and/or the editor(s) disclaim responsibility for any injury to people or property resulting from any ideas, methods, instructions or products referred to in the content.